Atmospheric clusters to nanoparticles: Recent progress and challenges in closing the gap in chemical composition

James N. Smith[a,*], Danielle C. Draper[a], Sabrina Chee[a], Michelia Dam[a], Hayley Glicker[a], Deanna Myers[a], Adam E. Thomas[a], Michael J. Lawler[a], Nanna Myllys[a,**]

[a] *Department of Chemistry, University of California, Irvine, CA USA*

Abstract

Aerosol nanoclusters (AN), defined here as molecular aggregates suspended in a gas with dimensions between 2 and 10 nm, are the link between substances that we think of as molecules, or the "gas phase," and those that we consider as particles, or the "condensed phase." The ability to measure and model the physical and chemical properties of size-resolved AN, which at present is rudimentary at best, is crucial for understanding how particles form and evolve in a number of environments that are natural or influenced by human activities. This review describes the current state-of-the-art for measuring and modeling the size-resolved composition of atmospheric AN. We focus specifically on instruments, many relying on mass spectrometry, that show promise for closing the measurement gap under atmospherically relevant conditions by increasing the size of measurable gas-phase clusters (bottom-up approaches) and by decreasing the size of measurable nanoparticles (top-down approaches). Theoretical methods for predicting AN composition have similarly relied on bottom-up approaches that extend the accuracy of quantum chemistry calculations to larger molecular systems, as well as top-down approaches that correct bulk composition aerosol models for size-dependent properties such as viscosity and volatility. Current measurement and modeling challenges that must be overcome in order

---

[*] jimsmith@uci.edu

[**] nanna.myllys@uci.edu

to close the gap are discussed.

Keywords: aerosol nanocluster, nucleation, new particle formation, nanoparticle composition

---

1. Introduction

Aerosol particles smaller than 10 nm in diameter, referred to here as aerosol nanoclusters (AN, Figure 1), play a unique role in the processes that link atmospheric chemistry to climate. Particles often begin their life in the atmosphere as nanometer-sized clusters by a process known as nucleation (Seinfeld et al., 1998). Instruments that directly measure the composition of ambient nucleated clusters (Jokinen et al., 2012; Junninen et al., 2010; Zhao et al., 2010) up to sizes of ∼2 nm suggest important roles for acid–base chemistry involving inorganic acids, such as sulfuric acid, methanesulfonic acid, and nitric acid, with ammonia and amines (Xu et al., 2017; Liu et al., 2018b; Wang et al., 2020; Zhao et al., 2010; Yao et al., 2018), and the direct condensation of low volatility halogen-containing compounds (Sipilä et al., 2016) and organics (Bianchi et al., 2016), all of which are enhanced by ion-mediated processes (Wagner et al., 2017; Rose et al., 2018). Once formed, these clusters can can grow into aerosol particles with diameters exceeding tens of nanometers, thus potentially serving as cloud condensation nuclei (CCN) (Kerminen et al., 2018; Kuang et al., 2009). Instruments that directly measure the composition of particles larger than ∼10 nm in diameter (Voisin et al., 2003; Smith et al., 2004; Wang et al., 2006), show them to be a heterogeneous mixture of binary and ternary salts (Smith et al., 2010) and complex organic compounds (Lawler et al., 2018). Water is a key, yet poorly understood, participant both in atmospheric nucleation and the subsequent growth of clusters into nanoparticles (Kulmala, 2003). Between 2 and 10 nm, in the size range of AN, lies a theoretical and observational "blind spot."

Field measurements show why it's important to understand the composition of ambient 2–10 nm diameter AN. Figure 2 shows Γ, defined as the ratio of observed particle growth rate to modeled growth rate from the condensation of

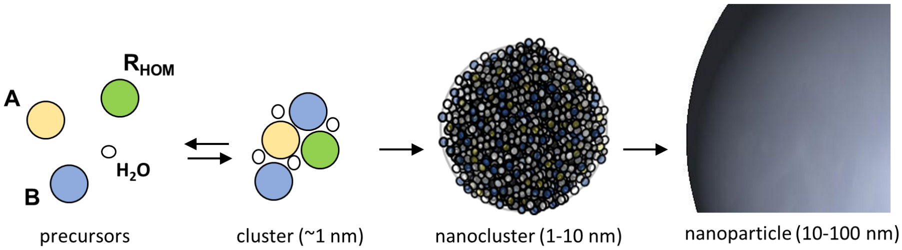

Figure 1: Schematic of the formation and evolution of atmospheric aerosol nanoclusters and definition of relevant size ranges. Precursor vapors are indicated accordingly: A: acid, B: base, R_{HOM}: highly oxygenated molecules

H_2SO_4 alone, for a new particle formation (NPF) event in Boulder, CO, at a site located downwind of a coal-fired power plant (Kuang et al., 2011). The event began with the production of 1 nm particles, and the x-axis represents the peak of the nucleation mode during the NPF event, with the starting and ending time of the growth event indicated on the plot. Overall, $\Gamma > 1$, which means that the observed growth rate of newly formed particles is greater than that which can be explained solely by the condensation of H_2SO_4. This appears to be generally true wherever NPF is observed: the exact species and mechanisms that are responsible for this growth enhancement are not well understood. In addition, there is a size-dependence to Γ, and that size dependence typically occurs in the diameter range of AN.

Numerous other mysteries can be solved with measurements of AN composition. Recent observations of NPF in Chinese megacities concluded that the theoretical survival probability of particles from 1.5–3 nm in diameter is practically zero due to high scavenging rates (Kulmala et al., 2017) — indeed, the size range between 1.5 and 10 nm has been referred to as the ”valley of death” for nucleated clusters (Wang et al., 2020). Direct measurements of AN composition are essential for understanding and ultimately predicting how nucleated clusters grow on this treacherous path to climate relevance.

This review article presents the state of the science in closing the measurement and modeling gap that currently exists for atmospheric AN composition.

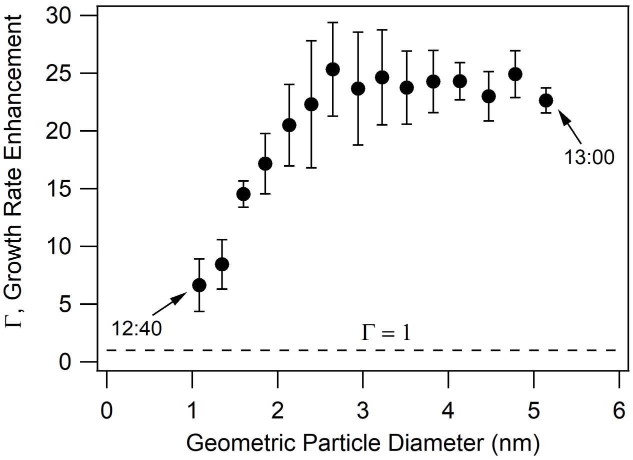

Figure 2: Size-resolved Γ (GR_{obs}/GR_{H2SO4}) for a new particle formation event observed in Boulder, CO, on 19 September 2010 starting at 12:40 and ending at 13:00, local time. Data from Kuang et al. (2012), used with permission. $\Gamma = 1$ also shown on plot for reference.

A related review reflects on the state-of-the-art in measuring size and concentration of particles in this size range (Kangasluoma et al., 2020). We will not focus on current understanding of atmospheric nucleation and NPF, both of which have been the subject of several recent reviews (Kerminen et al., 2018; Kulmala et al., 2014; Zhang et al., 2012). We begin with the current state of atmospheric AN measurements and continue with a similar discussion of the state of AN modeling. Each section covers the size range of interest (2–10 nm) from both directions: (a) from the bottom-up, in which we discuss the extension of measurements and models above the 1 nm diameter that is already routinely studied, and (b) from the "top-down," in which measurements and models are applied to diameters smaller than 10 nm by optimizing particle sampling and by introducing size-dependent corrections for properties such as volatility. Challenges and opportunities are discussed in each respective section. Finally, our review concludes with a perspective on the future hope that this observation and modeling gap may someday be closed.

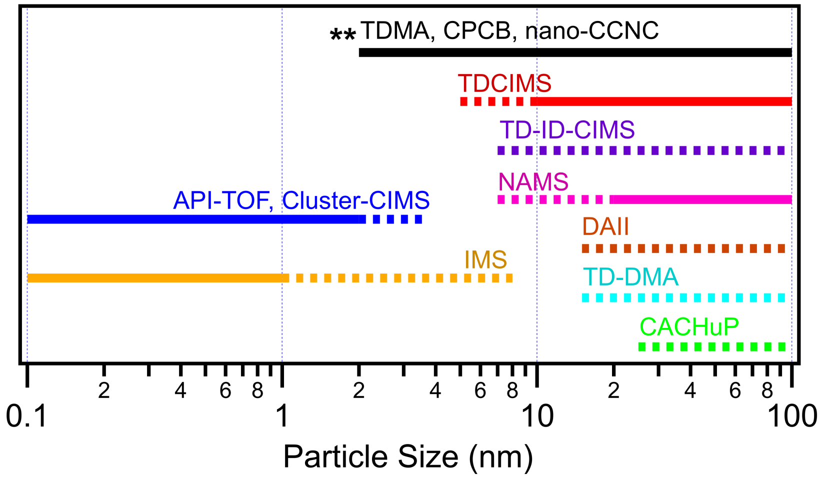

Figure 3: Overview of the diameter range for instruments that can perform size-resolved AN composition measurements. Solid lines indicate the sizes the instrument has measured in the field, while dotted lines indicate lab experiments. Instruments with asterisks (**) do not measure composition, but measure physical properties of AN that can infer AN composition.

2. Atmospheric aerosol nanocluster measurements

Figure 3 provides an overview of the measurements that show promise for obtaining size-resolved composition of atmospheric AN along with current size ranges that have been reported in the literature. This section focuses specifically on instruments that provide size-segregated composition with sufficient sensitivity as to allow them to be applied to atmospheric conditions. Most of these methods have already been used to make ambient observations. However some have thus far been confined to the lab and we present these insofar as we feel that their application to ambient measurements is possible.

2.1. Bottom-up approaches: Measuring super-nm atmospheric clusters

Bottom-up approaches take techniques traditionally used for sub-nm gas-phase molecular or cluster identification and quantification and expand the measured size range to the super-nm. In order to characterize super-nm clusters, these techniques must have detectors that can characterize composition at these larger sizes, and they should preserve cluster composition by reducing decomposition or evaporation of clusters and fragmentation of individual molecules. Mass spectrometry is frequently used to determine sub-nm atmospheric composition, and with advances in instrumentation in recent years, super-nm clusters are increasingly within reach. High sensitivity can be achieved by directly sampling ambient ions and making inferences for ambient neutral molecules and clusters. Alternatively, chemical ionization mass spectrometry has provided key measurements of ambient neutral species. Additionally, mobility-based approaches, often employing mass spectrometers as ion detectors, can reduce instrumental artifacts and help preserve cluster composition during sampling.

2.1.1. Time-of-flight mass spectrometry (TOF-MS)

Time-of-flight mass spectrometry (TOF-MS) is the most widely used technique for determining cluster composition under atmospherically relevant conditions. In particular, the atmospheric pressure interface TOF-MS (APi-TOF-MS), first described in Junninen et al. (2010) and now a commercially available instrument manufactured by Tofwerk AG, has been deployed to make ambient measurements in numerous locations around the world (Jokinen et al., 2012; Bianchi et al., 2016; Kürten et al., 2016; Sipilä et al., 2016; Sarnela et al., 2015; Yao et al., 2018). ANs are likely to be composed of an enormous number of atmospheric constituents including multiple permutations with the same nominal mass. For this reason, the high mass resolution, high sensitivity, and large mass range achievable by TOF-MS detectors make them invaluable for ambient measurements compared to quadrupole mass spectrometers, which generally feature similarly high sensitivity but lower mass range and resolution. The APi-TOF-MS has been used to detect ambient compounds with mass as high as 2 kDa (Sipilä et al., 2016), and this range has been extended to 20 kDa in laboratory studies (Renzler et al., 2017). There is not a uniform relationship between atomic mass and diameter, since the shape and size of a molecule is not directly related to its mass, but for globular molecules such as proteins 2 and 20 kDa correspond to spherical equivalent diameters of 1.5 and 3.6 nm, respectively (Erickson, 2009).

The APi-TOF-MS is able to directly measure ambient ions in the atmosphere, and inlet modifications including chemical ionization allow for direct measurement of neutral clusters (Bertram et al., 2011). Chemical ionization mass spectrometry (CIMS) introduces a reagent ion (e.g. ${NO_3}^-$, I^-, ${C_2H_3O_2}^-$, H_3O^+) to the sampled air flow, which will form sample ions via reaction or clustering according to their chemical properties. Often, this preserves molecular composition without fragmentation. Application of CIMS using ${NO_3}^-$ reagent ion to key atmospheric species such as sulfuric acid was first reported by Eisele & Tanner (1993), and more recently this was optimized for detecting ambient gas phase clusters in an instrument called Cluster CIMS (Zhao et al., 2010). Jokinen et al. (2012), adapted the Eisele and Tanner inlet design to the APi-TOF-MS to create the CI-APi-TOF-MS, with a limit of detection on the order of 10^4 molec cm^{-3} and the high mass resolution necessary to separate larger clusters of interest from interfering ambient compounds. These instruments regularly detect species like sulfuric acid, ammonia, amines, and highly oxygenated molecules (HOMs). A few notable AN cluster composition measurements include a complex mixture of sulfuric acid, ammonia, HOMs, and iodic acid in the free troposphere of the Swiss Alps (Bianchi et al., 2016), the domination of sulfuric acid-ammonia clusters in Antarctica (Jokinen et al., 2012), and iodic acid-containing clusters along the coast of Ireland (Sipilä et al., 2016). Figure 4 shows measurements of neutral cluster composition from the Sipilä et al. (2016) study, demonstrating the ability of the CI-APi-TOF-MS to resolve cluster composition to 2200 Th (equivalent to 2.2 kDa for these singly-charged ions).

2.1.2. Mobility-based approaches

Mobility-based approaches such as ion mobility spectrometry (IMS) or differential mobility analysis (DMA) can be coupled to mass spectrometers for mass detection and therefore are valuable bottom-up techniques for characterizing AN composition. Separation by ion mobility is effective for a wide range of size and composition measurements since it does not rely on chemical separation

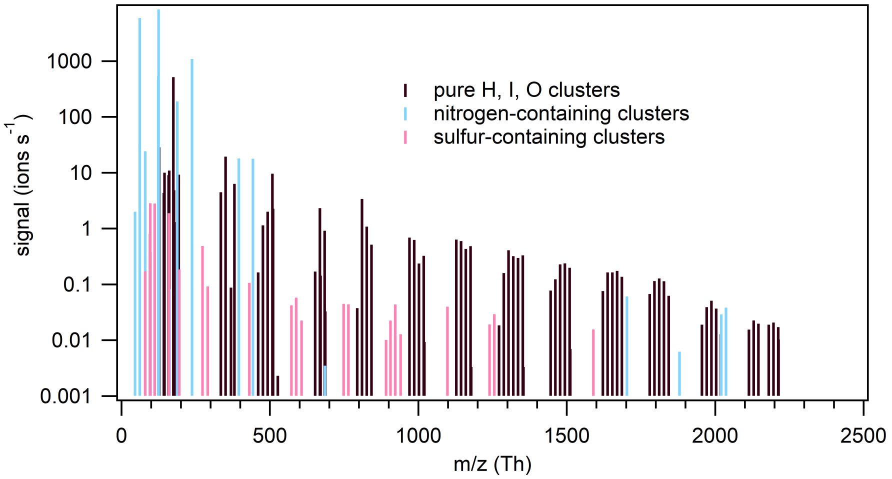

Figure 4: CI-APi-TOF-MS measurements of atmospheric composition during a NPF event in Mace Head, Ireland. The measurements demonstrate the important role of iodine oxide vapor partitioning in the production of AN in this locale. Data from Sipilä et al. (2016), used with permission.

.

(e.g. interaction with solvents or a stationary phase). Ion mobility is sensitive to molecular geometry, enabling it to separate isomers and other species that are similar in mass, which is one of the challenges of mass spectrometry, especially as ion mass-to-charge ratios are increased (Krechmer et al., 2016). For AN measurements in particular, DMA-based separation may provide an extra advantage over typical IMS drift tubes since they operate at atmospheric pressure, near room temperature, and with a variety of carrier gases (Oberreit et al., 2015), which can result in higher cluster stability under atmospherically-relevant conditions.

IMS-MS and DMA-MS have been shown to be powerful tools for measuring AN properties in laboratory experiments and an IMS-MS instrument has also been successfully deployed in the field (Krechmer et al., 2016). Laboratory experiments using DMA-MS have characterized properties such as density, collision cross section, cluster stability, and extent of hydration for sulfuric acid-dimethylamine nanoclusters ranging from 2-8.5 nm (Ouyang et al., 2015; Thomas et al., 2016) as well as for smaller iodine pentoxide-iodic acid clusters (Ahonen et al., 2019). An IMS-MS with a NO_3^- chemical ionization source was deployed to make ambient measurements during the Southern Oxidant and Aerosol Study (SOAS). AN measurements were not reported from this study, due at least in part to the relatively high condensation sink at this site and few new particle formation events (Lee et al., 2016). However, the authors did perform collision-induced dissociation (CID) analysis, applied between the IMS drift cell and TOF-MS, which allowed them to identify whether measured C_{20} dimers were covalently bound or more weakly bound clusters. This analysis demonstrates the ability of IMS measurements to provide size-separation of AN, which combined with CID allows for mass spectrometers that operate over a smaller mass range to still provide useful insights into composition.

2.1.3. Bottom-up measurement challenges and opportunities

The ability of mass spectrometry-based methods to detect super-nm atmospheric clusters is limited by the size-dependent detection efficiency of the system as well as the extent to which the instrument preserves molecular composition. With regards to the former, expansion into the AN size range can be achieved but requires instruments that combine high mass detection with an exceptionally high resolution needed to resolve molecular composition based on exact mass determination (Lössl et al., 2014). This is an area of rapid progress because of the interest in characterizing proteins, viruses, and other nanoscale biological structures; however, it is important to stress that direct measurements of AN mass are not likely to significantly close the measurement gap in composition. The latter point is discussed in detail in Section 4. It is worth noting that much of the foundational work in measuring ANs, including the earliest atmospheric ion measurements and the development of the cluster CIMS inlet, was done using a quadrupole mass spectrometer (Eisele, 1989; Eisele & Tanner, 1993; Eisele et al., 2006). As such, it may be beneficial to revisit some of those original experimental ideas and measurement sites with today's improved mass spectrometry approaches.

Quantification of cluster composition is a challenge for all mass-spectrometry-based approaches. The use of chemical ionization can lead to charging-induced fragmentation reactions, can create clusters within the ion source via ion-induced nucleation, and can introduce biases due to variations in ionization efficiency (Zhao et al., 2010; Kurtén et al., 2011; Ortega et al., 2014; Hyttinen et al., 2018; Iyer et al., 2016; Sipilä et al., 2015; Kupiainen-Määttä et al., 2013). Computational chemistry has provided many insights into these effects, but additional studies are needed given the diversity of sampled species and reagent compounds currently in use. Additionally, many compounds, most importantly water, may evaporate from the clusters during sampling and clusters themselves may decompose inside the vacuum of a mass spectrometer, leading to significant biases. To study collision-induced cluster fragmentation, Zapadinsky et al. (2019) developed a model that simulates the collision of a cluster with carrier gas molecules as it moves through the chambers of a mass spectrometer under an electric field and Passananti et al. (2019) applied the model to an APi-TOF mass spectrometer and systematically measured the effect of the applied voltages on the cluster fragmentation. Such modeling studies could be essential in efforts to extend bottom-up measurement techniques to super-nm atmospheric clusters.

2.2. Top-down approaches: Measuring sub-10 nm nanoparticle composition

Top-down approaches involve instrumentation that has been shown to effectively measure size-resolved ambient nanoparticle composition and pushes the size limit into the sub-10 nm range. Since mass scales as the particle radius cubed, one of the main challenges for top-down measurements of AN is isolating them from larger particles or else the signal will be overwhelmed by even a few large particles. Instrument sensitivity can also be a significant challenge for the low sample masses typically encountered for AN in ambient air and the potential contamination of samples from low-volatility gases. Currently, several approaches have been developed for obtaining nanoparticle chemical composition by: a) offline collection and analysis techniques; b) real-time, online detection using approaches that indirectly infer composition; c) using online detection with mass spectrometry-based direct composition approaches. In this section, these methods will be briefly described with emphasis on their ability to extend to diameters smaller than 10 nm.

2.2.1. Offline nanoparticle collection and analysis

The earliest measurements of the composition of the smallest particles in the atmosphere were made using offline approaches (Mäkelä et al., 2001), whereby particles are collected on a substrate in a size-segregated manner for later offline chemical analysis. As with all of the top-down approaches discussed, both collection and analysis of ANs and nanoparticles present challenges for offline methods.

Collection of nanoparticles and ANs in the atmosphere can be generalized to two main approaches: low-pressure cascade impactors and growth tube collection. The micro-orifice uniform deposit impactor (MOUDI) is perhaps the most common cascade impactor used for size-resolved particle collection in the atmosphere. The MOUDI is comprised of a series of rotating stages that sample particles on the basis of their aerodynamic diameter (Marple et al., 1991). While regular MOUDI collections typically do not extend below $\sim$ 50 nm (Kulkarni et al., 2011), the nano-MOUDI and similar low-pressure impactors (LPI) can sample particles as small as $\sim$ 10 nm aerodynamic diameter (Mäkelä et al., 2001; Wang et al., 2007), and another recently developed LPI was able to collect particles down to 7.7 nm (Arffman et al., 2014). Growth tube collection is another method that can help collect even smaller particles. The growth tube collector (GTC) collects particles as small as 5 nm by amplifying particle size by water condensation followed by impaction onto a collection stage or into a small volume of solvent (Hering & Stolzenburg, 2005). This technology has been commercialized into the sequential spot sampler (S3, Aerosol Devices, Inc.). The GTC on its own does not size-segregate collected particles, but can be used downstream of devices that size-select particles, as has been done in laboratory studies of 20 nm diameter particles Chen et al. (2018a). A class of devices related to the GTC are those that use water condensation to amplify particle size and aerodynamic lenses to concentrate the larger particles. The versatile aerosol concentration enrichment systems (VACES) is one instrument in this class, which can be combined with a MOUDI to enhance collection of sub-100 nm diameter particles (Geller et al., 2002, 2005).

Sample analysis might involve extraction or direct measurements of the constituents on the collection substrate. Solvent extraction can be paired with analysis such as ion chromatography or inductively coupled plasma mass spectrometry (Mäkelä et al., 2001). Additionally, illuminating the substrate with a light source to investigate optical absorption or the study of isolated particles on the substrate by microanalytical techniques such as secondary ion mass spectroscopy (SIMS) and Fourier transform infrared spectroscopy (FTIR) can be employed (Kulkarni et al., 2011). Imaging microscopy paired with elemental analysis has shown to be a key tool for offline analysis of ultrafine particles. Analysis of both lab-generated and field-measured nanoparticles via transmission electron microscopy and energy-dispersive X-ray spectroscopy can give insight into particle morphology and composition (Mäkelä et al., 2002). The latter spectroscopic approaches, which do not require sample preparation prior to analysis, have the benefit of minimizing sampling artifacts in measurements of particle composition.

2.2.2. Indirect online analysis

Indirect composition measurements of atmospheric nanoparticles can be made using tandem differential mobility analyzer (TDMA) techniques. Particles are size-selected and then exposed to a controlled environment, after which the resulting size distribution is measured to observe any size changes (Rader & McMurry, 1986). Most commonly, particles are conditioned with high relative humidity (RH) to investigate their hygroscopic properties (McMurry & Stolzenburg, 1989), high temperature to characterize volatility (Rader & McMurry, 1986), or saturated organic vapor to investigate organic composition (Joutsensaari et al., 2001; O'Dowd et al., 2002; Vaattovaara et al., 2005). Characteristic size changes resulting from the conditioning can be attributed to the presence of specific compounds, or classes of compounds, in the particles (McMurry et al., 1996; Kerminen, 1997). Since these TDMA approaches rely on the ability to size-select ambient particles, this approach has been successfully applied to obtain insights into AN composition (Sakurai et al., 2005; Wu, 2017). Figure 5 shows how the composition of particles larger than 3 nm was inferred through the combination of hygroscopicity and volatility TDMA measurements by Sakurai et al. (2005).

Another class of indirect composition measurements takes advantage of the dependence of aerosol particle growth dynamics on composition within condensation particle counters (CPCs), which also varies with the CPC working fluid. For example, a nano-cloud condensation nuclei particle counter (nano-CCNC) was developed to measure size-resolved hygroscopicity and thus infer chemical composition for 2–10 nm particles by scanning the water saturator temperature in a CPC (Wang et al., 2015). Growth characteristics within butanol-based CPCs have been employed to infer AN composition using a pulse height analysis technique to size butanol droplets that grow onto sampled AN as small as $\sim$1 nm in diameter (O'Dowd et al., 2002; Sipilä et al., 2009). Pairs of CPCs operated identically but with different working fluids have been used in a CPC battery (CPCB) to infer 2–20 nm AN water and butanol solubility (Kulmala et al., 2007). New methods of particle counting and size selection (Kangasluoma et al., 2020) ensure that these methods will continue to provide valuable information in the near-term.

2.2.3. Direct online analysis

The determination of molecular- or fragment-scale chemical composition for size-resolved aerosol by established real-time techniques is limited to sizes above around 40 nm for bulk measurements (Canagaratna et al., 2007) and around 120 nm or larger for single particle measurements (Murphy et al., 2006; Gard et al., 1997). Therefore efforts to probe molecular composition down to sizes on the order of 10 nm in a real-time or pseudo real-time manner have generally

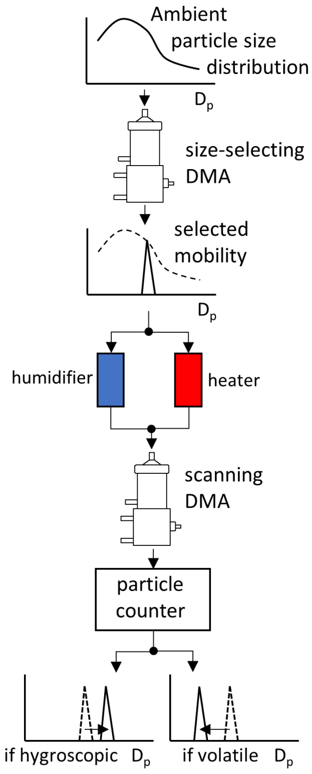

species	volatility (@100 °C)	hygroscopicity
sulfuric acid	volatile	very hygroscopic
sulfate	non-volatile	very hygroscopic
organics	intermediate volatility	slightly hygroscopic

Figure 5: Schematic of the operating principle of a Hygroscopicity/Volatility Tandem Differential Mobility Analyzer, including examples of indirect chemical properties that can be inferred from measurements. Diagram by H. Sakurai, used with permission.

relied on collecting picogram-scale particulate samples (over 1 million 10 nm particles) and then subsequently analyzing them once enough mass has been sampled for sufficient signal-to-noise.

Thermal desorption techniques comprise the majority of online instrumentation for nanoparticle composition. The original such instrument is the thermal desorption chemical ionization mass spectrometer (TDCIMS) (Voisin et al., 2003; Smith et al., 2004). TDCIMS employs unipolar particle chargers and differential mobility analyzers (DMAs) to size-select ultrafine particles for collection by electrostatic deposition onto a metal filament. After a period of collection, the sample is translated into a desorption and chemical ionization region, where the filament is resistively heated to volatilize sampled compounds by evaporation or thermal decomposition, depending on the compound and heating profile. The compounds volatilized and detected depend on the maximum temperature of the filament, melting and/or pyrolysis behaviors of the analytes, reagent ion chemistry, and the mass resolution of the detector. Contributions from low- and semi-volatile gas-phase species are accounted for and subtracted by alternating collection and background cycles, which differ only by whether high voltage is applied to the metal filament during the collection period.

The TDCIMS technique has been modified to adapt different sampling and ionization strategies. The Chemical Analyzer for Charged Ultrafine Particles (CAChUP) differs primarily in its use of a 70 eV electron ionization source rather than chemical ionization (Gonser & Held, 2013), with a smallest detectable particle size of 25 nm. Other implementations have thus far been applied to laboratory studies only. An ion drift (ID) tube was added to a TDCIMS-type instrument to create the TD-ID-CIMS, which benefits by having a controlled ion-molecule reaction time and thus a reduced need for chemical calibrations but has not yet been configured to measure size-resolved composition (Zhang et al., 2009). A similar conceptual approach to TDCIMS called the thermal desorption-differential mobility analyzer (TD-DMA) has been described recently by Wagner et al. (2018). The TD-DMA separates the sample volatilization region from the chemical ionization region and, in the application described, used a ${NO_3}^-$ CIMS reagent ion for detection of the desorbed compounds.

The smallest detectable particle size of the TDCIMS and similar techniques is determined primarily by sample mass, but the cubic dependence of mass on diameter and the higher diffusional loss rates of the smallest particles create challenges in extending the method into the AN size range. Practically, the smallest particle size that can be sampled by TDCIMS depends on the relative intensity and persistence of the smallest particles within measured aerosol populations. Size-resolved measurements of laboratory-generated particles can be

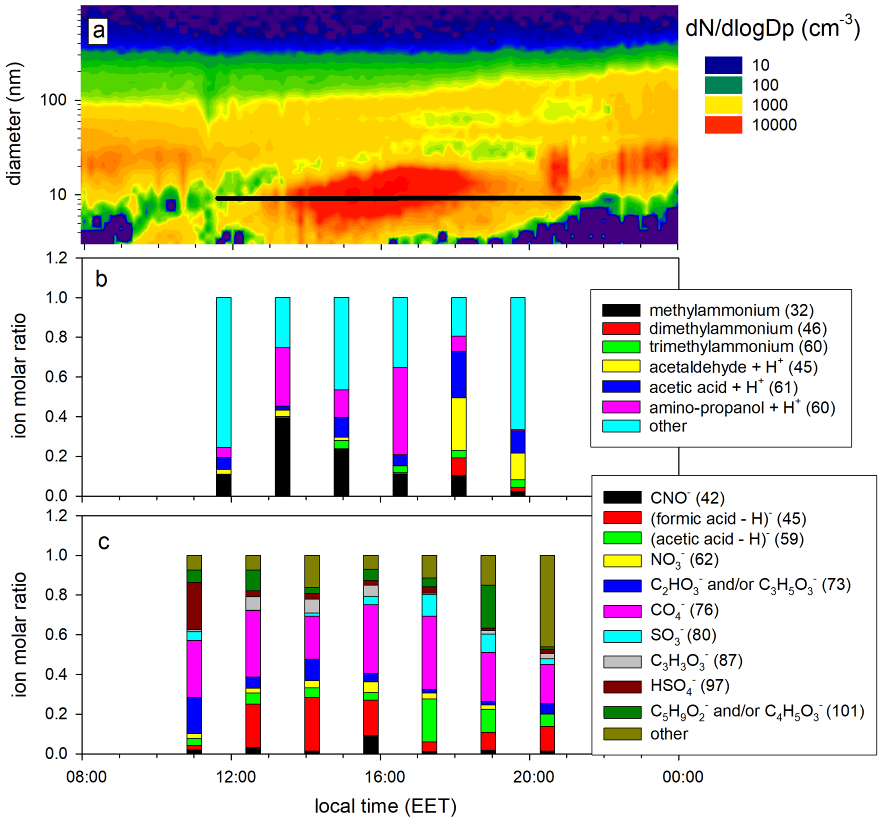

Figure 6: TDCIMS measurements of a new particle formation event in Hyytiälä, Finland on 9 April 2007 (Smith et al., 2010). Ion identifications are updated based on later high resolution TDCIMS measurements of 20–70 nm particles at the same site (Lawler et al., 2018). Alkylammonium and SO_3^- ions arise from thermal decomposition of the corresponding sulfate or bisulfate salts. The other ions primarily arise from thermal decomposition of larger oxidized organic molecules.

routinely performed on particles as small as 5 nm (Perraud et al., 2020a; Chen et al., 2018a). Persistent sub-10 nm ambient events are rare, but 8 nm particles have been analyzed in the Mexico City metropolitan area, and 10 nm particles were sampled in a boreal forest (Hyytiälä, Finland) (Smith et al., 2010). Figure 6 shows data from the forest measurements made during a unique NPF event on 9 April 2007 consisting of high concentrations of 10 nm particles ($> 10^4$ cm^{-3})

that grew very slowly (2.5 nm hr^{-1}) and persisted in the air for 8 hrs. The abundance of low molecular weight species is likely a combination of the lower mass range and resolution of the quadruple mass spectrometer used at the time as well as thermal decomposition of higher molecular weight species, the latter of which remains a challenge for analysis of organic species.

Under special conditions, it may be possible to extend the diameter range of thermal desorption techniques below 10 nm by bypassing size-selection and sampling bulk aerosols, effectively letting the atmosphere dictate sampled particle size. This is simply done in laboratory studies, where non-sized resolved instrumental approaches such as the filter inlet for gases and aerosols (FIGAERO) have been employed (Lopez-Hilfiker et al., 2014).

Laser desorption followed by mass spectrometry is another useful technique to measure the composition of size-resolved nanoparticles. The Rapid Single-Particle Mass Spectrometer (RSMS-II) measures composition of particles as small as ∼30 nm by employing a mechanism to selectively transmit a narrow particle size range into the focal point of a high-powered laser (Mallina et al., 2000). A successor to the RSMS-II, the nano-aerosol mass spectrometer (NAMS), measures elemental composition of particles in the size range of 7–150 nm (Wang et al., 2006; Horan et al., 2017b), though it has only been used in field measurements down to 20 nm (Pennington & Johnston, 2012). The NAMS charges particles with a unipolar charger and size-selection occurs via a tunable quadrupole digital ion guide. Several field adjusting lenses optimize particle capture in a downstream three-dimensional quadrupole ion trap, where a high-power Nd:YAG pulsed laser is used to vaporize trapped particles into singly- or multiply- charged atoms that are analyzed via reflectron time-of-flight mass spectrometry. The resulting mass spectra yield the elemental composition of individual sampled nanoparticles that is quantitative because the vaporization/ionization process is not subject to sensitivity biases due to molecular composition or matrix effects.

Although the NAMS has not yet made ambient measurements in the AN size range, such measurements are feasible in principle, and previous ambient nanoparticle measurements have provided unique compositional insights. Individual particle composition provides a snapshot of the internal vs. external mixing of particles. For example Zordan et al. (2008) shows evidence of both internal and external mixing in co-located and co-temporal nanoparticles during measurements in Wilmington, DE, indicative of diverse growth pathways happening in parallel. The quantitative nature of the NAMS technique enables mass-closure studies on gas-particle partitioning of key compounds such as sulfuric acid (Bzdek et al., 2012). The biggest challenge of elemental analysis for atmospheric particles is that molecular composition can only be inferred, which is especially difficult for organic species (Zordan et al., 2008; Bzdek et al., 2014; Stangl & Johnston, 2017).

Other mass spectrometry-based approaches include mobility separation combined with electrostatic precipitation-electrospray ionization mass spectrometry. This is a very gentle approach for volatilizing and ionizing collected aerosol components, but the detection limits are significantly higher than TDCIMS-type approaches (He et al., 2015). A technique that shows promise for molecular-scale composition analysis at roughly 10 nm sizes is mobility separation combined with droplet assisted inlet ionization mass spectrometry (DAII) (Horan et al., 2017a). Ih the DAII inlet, sampled nanoparticles nucleate liquid water droplets by exposure to supersaturated water vapor. Rapid heating of these droplets causes molecular ions to form by a gentle, electrospray-like process, and the resulting ions are detected by mass spectrometry.

2.2.4. Top-down measurement challenges and opportunities

The offline collection and analysis approach has a demonstrated potential to provide information on the composition of atmospheric nanoparticles, but several limitations would need to be addressed before this can be extended to AN composition. Collection methods must be immune to contamination by both low-volatility gases as well as from larger particles. Mobility-based separation, e.g. a size-selecting differential mobility analyzer, is one of the few approaches that can satisfy both requirements. Analysis of a 2002 NPF event in Atlanta, GA, shows that 10 nm charged particles can be size-separated by low-resolution mobility-based separation and delivered to a sampling device at a rate of 100–200 pg hr^{-1} (McMurry et al., 2009). If combined with water-based growth tube collection, this approach could supply up to a nanogram of 10 nm particles for the NPF event shown in Figure 6. This sample size, if extracted into 10 μl of solvent, requires offline approaches that have picogram sensitivities that, while challenging, can be achieved with electrospray mass spectrometry as well as a variety of other approaches (Hu et al., 2007; Visser, 2002; Fialkov et al., 2007; Allen et al., 1994; Kalberer et al., 2002). Research in improving the sensitivity of chemical analysis instruments is rapidly progressing, thus offline analysis should still be considered a viable approach for determining atmospheric AN composition.

Indirect online analysis approaches have limitations relating to the fact that chemical composition can only be inferred. Nonetheless, it is important to note that this is the only measurement that has already been demonstrated as capable of analyzing in the size-range of AN (2–10 nm diameter). Mobility-based separation as well as particle counting have undergone many improvements (Kangasluoma et al., 2020) but these have not yet been transferred to TDMA instruments. Thus we should not underestimate the potential contributions of indirect online analysis in our efforts to close the measurement gap from clusters to nanoparticles.

Direct online analysis has thus far been based on the mass spectrometric detection of molecular or elemental ions. In the case of the former, it is important to note that the sensitivity of sampling, ionization, and detection of molecular ions by chemical ionization mass spectrometry can vary considerably over the range of compounds found in atmospheric aerosol particles (Hyttinen et al., 2018). Additional experimental and theoretical work is needed to quantify detection biases in different chemical ionization approaches. In addition, thermal degradation of desorbed compounds needs to be better understood and mitigated in TDCIMS and related instruments. Both tasks are aided by the smaller class of compounds that are likely to be relevant to AN formation and growth. Recently, TDCIMS sensitivity increases were reported in laboratory measurements by replacing the radioactive foiled-based ion source design with a new design based on soft x-ray ionization (Perraud et al., 2020a), which opens up new opportunities for sub-10 nm measurements. The development of quantitative approaches such as NAMS should continue with a focus on sub-10 nm composition, ideally together with approaches such as TDCIMS that are not as quantitative but supply important molecular information. Finally, the ability of both NAMS and TDCIMS to detect AN is limited by the low efficiencies by which these small particles are charged. Unipolar particle chargers are typically employed, which produce a singly charged fraction of ∼0.1 for sampled 5 nm diameter particles (Smith et al., 2004). Attempts to increase the charged fraction to 1 in unipolar chargers are underway (Chen et al., 2019). Additional enhancement of charged AN has been reported using a "NanoCharger," a device that enhances both the charging efficiency and concentration of sampled sub-10 nm diameter particles for analysis by TDCIMS (Kreisberg et al., 2018). The combination of the NanoCharger and TDCIMS should be capable of efficiently analyzing particles as small as 4 nm in diameter, which would require a sampled flow rate of $\sim$100 L min^{-1}.

3. Atmospheric aerosol nanocluster modeling

Aerosol nanocluster formation and growth are closely linked to gas-phase chemistry, as the vapors that participate in these processes are typically oxidation products of atmospheric gases such as sulfur dioxide and volatile organic compounds. There exists a plethora of different condensable vapors and the partitioning of these depend on AN size, while condensed phase reactions that follow uptake can irreversibly alter the vapor pressure of these compounds. Temperature and RH have significant, and often non-linear, impacts on AN composition. This large parameter space creates significant challenges for process-level models that attempt to simulate AN formation and growth. In this section, we summarize the main theoretical approaches used to investigate the formation and evolution of AN.

3.1. Bottom-up approaches: Modeling super-1 nm atmospheric cluster composition

Bottom-up modeling approaches address the question: What is the most likely composition and structure of ambient molecular clusters? A proper answer to this question requires two interrelated steps. First, properties such as free energies must be solved for a set of clusters. This is made increasingly difficult as cluster size increases. In addition, a cluster dynamics calculation must be performed to determine its net formation rate under atmospherically relevant conditions. Explicit treatment of all possible combinations of atmospheric acids, bases, water, and oxidized organic compounds is not a reasonable goal, even with the most powerful supercomputers. For example, the boreal forest atmosphere can contain over 1000 possible pre-nucleating vapors and population dynamics simulations require cluster properties of up to 10 molecules, which would make an order of 10^{30} different cluster combinations. Because of this, most studies to date have focused on a key set of clusters that provide some insights into AN formation (Chen et al., 2012). In this section we review the methods currently in use for such simulations and assess their ability to be extended into the AN size range.

3.1.1. Cluster thermodynamics calculations

Theoretical approaches to obtain cluster thermodynamic properties can be classified into three categories depending on the scale at which the interactions between the nucleating compounds are treated: classical liquid drop models, force field methods, and electronic structure calculations. The simplest theoretical framework, the classical liquid drop model, treats clusters as spherical bulk-liquid droplets and requires as input only the liquid density, molecular mass, surface tension, and saturation vapor pressure of the compound (Vehkamäki & Riipinen, 2012). The free energy change in the formation of a one-component cluster with N molecules and saturation rate S can be written as

$$\Delta G = A\sigma - k_{\mathrm{B}}TN\ln S, \tag{1}$$

where A is the surface area of the cluster, σ is the surface tension, k_{B} is the Boltzmann constant, and T is the temperature. The first term is the energy cost of the surface formation and the second term represents the lowering of free energy when the molecules go from supersaturated vapor to liquid. The classical liquid drop model does not describe nano-sized systems well due to its reliance on bulk liquid surface tension and cluster sphericity (Merikanto et al., 2007; Vehkamäki, 2006).

Methods based on force fields such as classical molecular dynamics (CMD) are used to describe the interactions between molecules in terms of their functional groups (Car & Parrinello, 1985). The basic premise of these methods is that the interactions in a molecular system can be described in simple terms without explicitly accounting for quantum mechanical effects. A typical CMD force field includes bonded interactions (bond stretching, angle bending, and torsional distortion) and non-bonded interactions (electrostatic and van der Waals) (Lifson & Warshel, 1968; Allinger, 1977). CMD methods have been used to simulate many physiochemical phenomena such as ice nucleation on silver iodide particles (Roudsari et al., 2020), interactions between sulfuric acid and water in stable clusters and at a planar liquid–vapor interfaces (Toivola et al., 2009), and collisions between pre-nucleating vapors (Halonen et al., 2019). Since CMD methods do not allow for bond formation or breaking, their application to describing the structure, energy and dynamics of atmospheric clusters is far from straightforward. Most atmospherically important clustering processes involve proton transfer reactions requiring quantum mechanical treatments. In the most advanced *ab initio* molecular dynamics (AIMD) approaches, atomic nuclei are treated according to classical mechanics while the electrons are treated explicitly by quantum chemical methods and the energy is calculated on-the-fly at each step of the simulation. As AIMD approaches allow the covalent bond to break and form, they have been successfully applied to study proton transfer reaction dynamics and sample the potential energy surfaces of reactive clusters (Loukonen et al., 2014; Xu et al., 2017; Kumar et al., 2018).

The critical cluster size in atmospheric nucleation may be surprisingly small and is thus treatable by high-level quantum chemistry methods. The actual vapor concentration-dependent Gibbs free energies for each cluster can be obtained from the quantum chemical Gibbs free binding energy and vapor concentrations through the law of mass action:

$$\Delta G(P_1, P_2, ..., P_n) = \Delta G(P_{\mathrm{ref}}) - k_{\mathrm{B}}T \sum_{i=1}^{n} N_i \ln \frac{P_i}{P_{\mathrm{ref}}}, \tag{2}$$

where P_i is partial pressure of component i in the vapor phase, N_i is the number of molecules of type i in the cluster, and n is the number of components in the cluster. Density functional theory (DFT) has been the dominant quantum chemistry method to study cluster formation due to its reasonable computational cost. Commonly used density functionals in past atmospheric cluster studies have included ωB97X-D, PW91, M06-2X and B3LYP-D3 (Nadykto et al., 2011; Xu et al., 2018; Gale et al., 2020; Elm et al., 2012, 2016; Zhang et al., 2017; Leverentz et al., 2013; Kumar et al., 2018; Kurtén et al., 2007). While DFT has been shown to provide good structures and thermochemistry, electronic energies may be inaccurate (Elm & Mikkelsen, 2014; Elm et al., 2015; Ortega et al., 2008). A common solution to this is to perform optimization and frequency calculations using DFT and use highly correlated wave function methods such as Møller-Plesset or coupled cluster theory to correct electronic energies. Different multi-step approaches have also been used to investigate cluster formation and gas-phase reactions (Ortega et al., 2008, 2012; Henschel et al., 2016; Olenius et al., 2017).

The recent development of reduced scaling approximations has significantly increased the applicability of highly correlated quantum chemical methods such as MP2, CCSD and CCSD(T) to modeling cluster composition. Those methods have previously been restricted to benchmarking the smallest systems containing a maximum of a few atoms or a few tens of electrons due to the high computational cost and poor scaling. One example to lower computational time is the resolution-of-identity approximation which reduces the total computational cost by about an order of magnitude and only introduces minor errors into the calculation, thus its use is strongly recommended (Neese, 2003). Perhaps the main advance in gaining accurate energy description with low computational cost is the development of local electron correlation approaches. The goal of local correlation methods is to reduce the scaling with system size, ideally to linear scaling, without sacrificing the intrinsic accuracy of the calculation. Riplinger et al. (2013, 2016) developed a domain-based local pair-natural orbital (DLPNO) approximation, which can result in linear scaling and still produce the accuracy of their canonical counterparts. Benchmark studies have shown the DLPNO–CCSD(T) method to be a reliable and affordable way to study atmospheric processes such as the formation of salt particles, the hydration of clusters and chemical reactions on cluster surfaces (Myllys et al., 2016a; Elm et al., 2017a; Kildgaard et al., 2018a; Hirvonen et al., 2018; Elm & Kristensen, 2017).

The determination of a global minimum cluster structure is a significant challenge that can lead to an erroneous description of cluster composition and stability. There is no foolproof method to locate a global minimum cluster structure from a complex potential energy surface, thus many different sampling techniques have been developed. Past atmospheric cluster studies have employed, for instance, simulated annealing (Kirkpatrick et al., 1983; Loukonen et al., 2010; Day et al., 2000), basin hopping (Hartke et al., 1998; Temelso et al., 2018a), artificial bee colony algorithm (Zhang & Dolg, 2015, 2016; Zhang et al., 2020; Kubečka et al., 2019; Li et al., 2017), and Fibonacci sphere (González, 2010; Kildgaard et al., 2018a,b). While the main task of a configurational sampling technique is to find the global minimum structure, several local minima can be used to obtain more accurate thermochemistry. The effect of accounting for multiple minimum structures has been tested for sulfuric acid hydrates and oxidized organic compounds containing clusters (Temelso et al., 2012; Partanen et al., 2016), and the error caused by the single structure approximation is modest even for nanometer-sized clusters (lowering the free energy less than

1 kcal/mol) (Partanen et al., 2016; Kubečka et al., 2019; Rasmussen et al., 2020). Therefore, this correction is usually not worthy of additional computational time.

A common assumption is that the molecular clusters vibrate harmonically about their equilibrium geometries and rotate rigidly as a single entity. This rigid rotor–harmonic oscillator (RRHO) approximation may lead to large errors in Gibbs free energy. As anharmonic calculations are limited to the smallest clusters due to the computational restrictions, anharmonic scaling factors can be used to at least partially correct errors caused by vibrational anharmonicity. Temelso & Shields (2011) estimated the role of anharmonicity in hydrogen-bonded water clusters by calculating scaling factors using the vibrational perturbation theory, VPT2. They showed that intermolecular bonds are normally more anharmonic than intramolecular bonds, which demonstrates the importance of separating the modes into different classes. While the anharmonic effects lower the Gibbs free formation energy substantially, the energetic ordering of different isomers remains the same (Temelso et al., 2011). Additionally, in weakly-bound molecular clusters, some molecules might experience internal rotation. This high-amplitude motion leads to low-lying frequencies, which may cause large errors to the entropy description. That error can be partly corrected by removing or shifting frequencies below some cut-off value or by the so-called quasi-harmonic approximation (QHA), in which the lowest frequencies are treated as free rotors (Grimme, 2012). The difference between RRHO and QHA increases nearly linearly with system size and it can be up to several kcal mol^{-1} for a nanometer-size clusters (Myllys et al., 2016b). In addition, quantum chemistry programs might not be able to correctly recognize molecular symmetry, which causes an error in the entropy calculation. The effect of including correct symmetry numbers is roughly equal but opposite to the effect of QHA (Besel et al., 2020). Using anharmonic scaling factors, QHA and correct symmetry numbers does not require additional computational power, so they can be used for any cluster size.

Applicability of quantum chemical methods can roughly be divided into three parts: small dimers, medium-sized clusters and super-nm particles. To accurately study dimer properties, canonical coupled cluster energies, such as CCSD(T)-F12/cc-pVTZ-F12, can be used together with anharmonic thermochemistry, which can for instance be calculated by VSCF at the MP2-F12/cc-pVTZ-F12 level of theory to yield the most accurate properties, energy descriptions, and even anharmonic potential energy surfaces (Partanen et al., 2012, 2013). For clusters up to 1.5 nm in size, roughly 10 molecules, an increasingly popular approach has been DLPNO–CCSD(T)/aug-cc-pVTZ//ωB97X-D/6-31++G**, and together with Elm et al. (2020), we recommend this as the standard level of theory in cluster calculations. The benefit of having a universally applied approach is to be able to compare results worldwide between different research groups. When particle size increases, DFT can be applied to gain at least qualitative level information of particle formation and properties. Benchmark studies have shown that ωB97X-D has a superior performance for hydrogen-bonded clusters and it is suggested to apply for system sizes for which highly correlated methods are out of reach (Schmitz & Elm, 2020). A PW91 functional also offers a good compromise between cost and efficiency. Elm (2019) used PW91/6-31++G** level of theory to study clusters containing sulfuric acid and an oxidized organic compound, MBTCA, up to cluster size of 2.2 nm. Thus, density functional theory can be applied to model the composition of the smallest AN. For calculations that extend to systems several nanometers in size, semiempirical approaches can be explored. However, one should be careful as parameterized methods might lead to qualitatively wrong descriptions when the studied system does not behave consistent to the empirical parameter space.

3.1.2. Cluster population dynamics simulations

There are two main approaches for relating cluster thermodynamics to the cluster distribution under atmospheric conditions. The historical approach, classical nucleation theory (CNT), uses bulk liquid properties to predict cluster thermodynamics and solves analytically the birth–death equation leading to a net rate at which critical clusters are formed (Vehkamäki, 2006). A common example of the failure of CNT is that it predicts binary sulfuric acid–water nucleation rate to be over 10 orders of magnitude lower than observations (Yue & Hamill, 1979). Thus it is clear that a more sophisticated approach that relies on thermodynamics derived from first principles is needed to accurately model nucleation. Thermodynamics obtained from quantum chemistry provides insights into cluster stability, but the prediction of AN formation and growth rates requires modeling the kinetics of a population of interacting clusters. From a kinetic perspective, high evaporation rates lead to thermodynamic barriers and clusters that have not yet overcome the barrier and tend to evaporate faster than the rate by which they collide with vapor molecules. The evaporation coefficients of the clusters can be obtained from the Gibbs free binding energies of the evaporating cluster $(i + j)$ and its products i and j as

$$\gamma_{(i+j)\to i,j} = \beta_{i,j} \frac{P_{\mathrm{ref}}}{k_{\mathrm{B}}T} \exp\left(\frac{\Delta G_{i+j} - \Delta G_i - \Delta G_j}{k_{\mathrm{B}}T}\right), \tag{3}$$

where P_{ref} is the reference pressure, k_{B} is the Boltzmann constant, T is the temperature, and ΔG is the Gibbs free binding energy. The collision coefficients $\beta_{i,j}$ can be obtained most simply from kinetic gas theory or more accurately by taking into account long-range intermolecular forces. Yang et al. (2018) developed a collision rate theory–molecular dynamics simulation approach and calculated condensation and dissociation rates for gas phase metal clusters. Using molecular dynamics simulations, the effect on collision coefficients caused by molecular interactions has been studied and found to be enhanced by 2.2 for neutral sulfuric acid molecules compared with kinetic gas theory (Halonen et al., 2019). For collisions between charged and neutral species, the effect is much larger, on the order of 10-fold compared with hard-sphere collision coefficients (Leppä et al., 2013).

The time evolution of a cluster population is described by the birth-death equation, i.e., discrete general dynamic equation (GDE), which is written for each cluster as

$$\frac{dC_i}{dt} = \frac{1}{2}\sum_{j<i}\beta_{j,(i-j)}C_jC_{(i-j)}+\sum_{j}\gamma_{(i+j)\rightarrow i,j}C_{(i+j)}-\sum_{j}\beta_{i,j}C_iC_j-\frac{1}{2}\sum_{j<i}\gamma_{i\rightarrow j,i-j}C_i+S_i-L_iC_i, \tag{4}$$

where C_i is the concentration of cluster i, $\beta_{i,j}$ is the collision rate coefficient between i and j, $\gamma_{(i+j)\rightarrow i,j}$ is the evaporation rate coefficient of cluster $(i+j)$, S_i is an external source term, and L_i is an external loss term corresponding to coagulation onto pre-existing surfaces. The positive terms correspond to all collision and evaporation processes that create cluster C_i, and the negative terms to all processes where the cluster is lost. The birth-death equations are implemented in models such as the Atmospheric Cluster Dynamics Code (ACDC) and have been widely used to study particle formation (McGrath et al., 2012). Applications have included the clustering of oxidized organic compounds (Elm, 2019), the role of various bases in sulfuric acid-driven particle formation (Olenius et al., 2013; Xie et al., 2017; Myllys et al., 2018, 2019b; Ma et al., 2019), the formation of nitric acid-containing clusters (Liu et al., 2018b; Chee et al., 2019), the effect of methanesulfonic and methanesulfinic acids in clustering (Shen et al., 2019; Ning et al., 2020), and the role of hydration in particle formation (Henschel et al., 2016; Olenius et al., 2017; Liu et al., 2018a). Figure 7 shows an example of the step-by-step cluster growth pathways for a system containing compounds A and B that can be achieved with ACDC. The system grows via an additions of heterodimer AB to the cluster or sequential additions of compound A and subsequently compound B. The compositions of steady-state clusters is close to the A:B ratio of 1:1. It should be noted that the cluster composition might not be same as AN composition and one should combine bottom-up and top-down approaches to get insights of AN compositions (Chen et al., 2018b; Chee et al., 2019) Cluster growth and composition are strongly dependent on participating compounds, their concentrations and temperature.

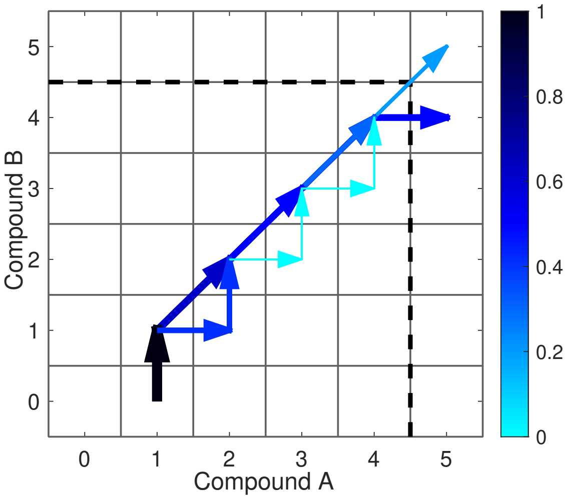

Figure 7: Illustrative example of the main cluster growth pathways for a two-component system. The x- and y-axes give the numbers of compounds A and B in the cluster and the color of the arrow indicates the relative flux at which each step is expected to proceed.

3.1.3. Bottom-up modeling challenges and opportunities

Cluster formation may also be hindered by kinetic barriers. This effect was studied by Bzdek et al. (2010a,b), who investigated the exchange of amines for ammonia in ammonium bisulfate and ammonium nitrate clusters using Fourier transform ion cyclotron resonance mass spectrometry. They found that displacement of the first few ammonia molecules by dimethylamine occurs with near unit efficiency, but when the cluster size increases an ammonium ion can be trapped in the center of the cluster, which hinders the base exchange. In AN the volume-to-surface ratio is larger than in clusters, thus more molecules will be trapped and only surface molecules are likely to undergo base exchange. While the current quantum chemical approaches mainly focus on cluster formation via global minimum structures, the actual clustering pathway might be slightly different due to kinetic limitations (DePalma et al., 2014a,b). Thus the role of kinetic barriers in atmospheric clustering should be better understood.

While the substitution of ammonia by amines is showed to be a favorable reaction, the co-presence of ammonia and amines has been shown to enhance nucleation more compared to ammonia or amine alone (Yu et al., 2012; Glasoe et al., 2015; Temelso et al., 2018b; Wang et al., 2018; Li et al., 2020; Perraud et al., 2020b). The reason for this synergistic effect is found in the cluster structures, where ammonia is more likely to be protonated than amine and likely to locate to the center of the cluster due to four possible hydrogen bonding sites (Myllys et al., 2019a). The atmosphere has many common emission sources for ammonia and amines, and thus synergistic effects might significantly impact nucleation and new particle growth, however this synergy is not well-understood or implemented in models. Systematic studies involving multiple compounds are needed to understand the role of synergistic effects in AN formation.

The atmospheric sources, abundance, and role of individual amines are relatively well-studied, however their oxidation mechanisms and the role of oxidation products in AN formation is a topic that can be explored further with computational approaches. It is known that amines undergo rapid oxidation in the atmosphere and products such as imines and amine oxides might participate in NPF (Angelino et al., 2001; Silva et al., 2008; Nielsen et al., 2011). Recent simulations have shown that some possible oxidation products, e.g. trimethylamine oxide, could play an important role even given the low levels expected in the atmosphere (Myllys et al., 2020).

In addition to the oxidized amines, another area that should be explored further with the approaches described above is the role of oxidized organic compounds. Xu & Zhang (2012) studied clusters consisting different dicarboxylic acids with sulfuric acid, ammonia and water. Based on the Gibbs free formation energies of the heterodimer and heterotrimer clusters, they suggested that dicarboxylic acids can contribute to the clustering process by binding to sulfuric acid and ammonia. Clustering mechanisms of several multifunctional organic compounds have been studied together with acids, bases, water and ions (Nadykto & Yu, 2007; Elm et al., 2017c; Arquero et al., 2017; Zhang et al., 2018; Myllys et al., 2017; Xu et al., 2010b,a; Ortega et al., 2016). Elm et al. (2017b) have found that carboxylic acids having at least three functional groups are the most likely candidates to be involved in clustering and that cluster formation from oxidized organic compounds might be unconnected to acid–base clustering pathways (Elm, 2019). It is particularly challenging to model the role of large HOMs in particle formation. For instance, covalently-bound dimers formed from monoterpene oxidation products contain ∼70 atoms, which makes clustering studies infeasible with accurate quantum chemistry methods (Bianchi et al., 2019; Draper et al., 2019). It has also been suggested that ions are needed to stabilize clusters consisting only of oxidized organic compounds (Kirkby et al., 2016). The large variability between results of different studies highlights the importance of further studies using computational chemistry of oxidized organic compounds in order to fully assess the role of these compounds in atmospheric AN formation.

The abundance of water vapor in the atmosphere exceeds that of other condensable vapors by 8–10 orders of magnitude and water is known to affect the particle formation process (Vaida et al., 2003; Vaida, 2011). However, water is most likely evaporating rapidly from the ions under high-vacuum conditions in mass spectrometers, so its connection to cluster formation is difficult to observe directly (Schobesberger et al., 2013). This makes this research area ideal for computational approaches, yet the treatment of water molecules is not straightforward. While as a small molecule water does not significantly increase computational time of a single free energy calculation, an extra molecule in the cluster structure presents an additional challenge to configurational sampling. Kildgaard et al. (2018a,b) have developed a systematic hydrate sampling technique that aims at allowing water to be explicitly treated in clustering studies. They have studied sulfuric acid–water clusters up to four sulfuric acid and five water molecules (Rasmussen et al., 2020).

3.2. Top-down approaches: Modeling sub-10 nm nanoparticle composition

Top-down approaches start with models that simulate the partitioning between gas and bulk phase and then account for size-dependent processes that alter bulk phase activity. An example of the latter is the significantly elevated equilibrium vapor pressures above highly curved surfaces, also known as the Kelvin effect. As stable clusters grow through the AN size range, they begin to resemble macroscopic matter and evaporation decreases for some compounds. From a theoretical point of view, top-down approaches begin with classical thermodynamics in which particles are treated as a continuous substance instead of discrete clusters. Solving the coupled, discrete GDEs in Equation 4 becomes computationally infeasible so continuous GDEs are used. The main difference between the discrete and continuous GDE approaches is that the continuous equations do not include stochastic effects related to molecular collisions and evaporation. Instead, condensational growth is given as a uniform flow of particles toward larger sizes determined by the growth rate, which becomes a justified approach as the particle size increases (Olenius et al., 2018). The main challenge in top-down modeling approaches relates to the treatment of this growth. Figure 8 demonstrates that growth involves many different processes, including evaporation as well as possible particle-phase reactions. Chemical reactions at the particle surface or in the bulk, such as so-called accretion reactions, can produce compounds that have a larger number of functional groups and high molecular mass (Barsanti & Pankow, 2004, 2005, 2006). These compounds are less volatile and capable of forming more stable particles than their reactants (Pankow & Asher, 2008; Hirvonen et al., 2018). In addition, the formation of organic salts via reactions of organic acids with base compounds are potential mechanisms for lowering the volatility of particle-phase organic compounds (Smith et al., 2010). An additional challenge is identifying the gas phase precursors and reactants that control growth. Various approaches have been used to model these processes by modeling them in a single, representative particle. We describe these approaches in this section.

3.2.1. Process-level models

The compounds driving the initial clustering, which includes sulfuric acid with various base compounds as well as organic vapors, may also be relevant to growth in the AN size range. In many environments, a major fraction of parti-

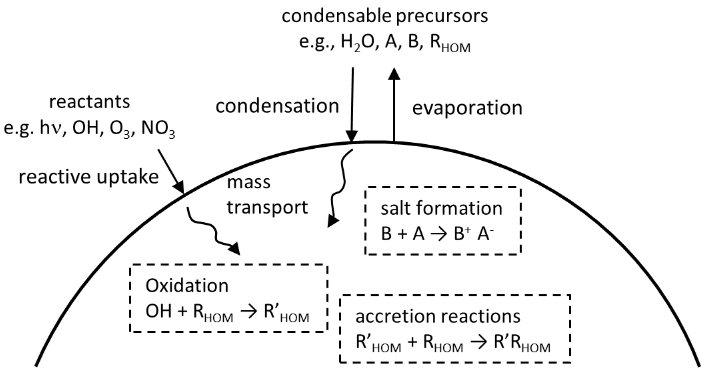

Figure 8: Schematic of the processes that control volume increase of a model particle. Acids (A), bases (B), highly oxidized molecules (R_{HOM}), and water, as well as other reactive species such as light and oxidants, partition into particles. Diffusive mass transport brings theses species into the bulk phase, where they may react by various mechanisms, three of which are presented above. Unreacted species as well as bulk and surface reaction products may stay in particles or evaporate.

cle growth is attributed to highly oxygenated molecules (HOMs), which may be formed from biogenic or anthropogenic volatile organic compounds. Combining a large diversity of precursors with a variety of possible oxidation pathways leads to an enormous number of possible oxidation products, most of which have not been confirmed by measurements. Therefore, alternative approaches to studying specific molecules must be used. Atmospheric organic compounds are often grouped by a volatility basis set (VBS), which is a simplified representation used when detailed information of the vapor properties is not available (Lane et al., 2008; Donahue et al., 2011, 2012). VBS describes compounds in terms of saturation concentrations and oxidation states that can be measured even if the compound is not known (Kroll et al., 2011). Saturation concentration is strongly dependent on temperature, meaning that a compound that mainly exists in particle-phase at low temperature can be mainly in gas-phase at higher temperature. In its simplest form, a single particle model incorporating the VBS framework assumes reversible condensation. More sophisticated approaches allow for particle phase reactions such as those shown in Figure 8, which create new species that re-partition based on their estimated vapor pressures.

The Model for Acid–Base chemistry in NAnoparticle Growth (MABNAG) utilizes detailed thermodynamics for calculations of particle-phase acid–base chemistry based on the bulk properties (Yli-Juuti et al., 2013). MABNAG assumes the particles to be aqueous solution drops, with condensing vapors that can contain both inorganic and organic compounds as well as water vapor. MABNAG relies on bulk thermochemical properties calculated using the Extended Aerosol Inorganics Model (E-AIM), with an assumption that the particle-phase is constantly in equilibrium with respect to acid–base chemistry during the particle growth (Clegg et al., 1992). MABNAG has been used to simulate sulfuric acid–dimethylamine–water particle growth and salt formation in multicomponent sulfuric acid–organic acid–base compounds particles (Ahlm et al., 2016; Yli-Juuti et al., 2013). Mohr et al. (2019) combined the VBS parametrization with MABNAG and studied the role of oxizided organic compounds with different saturation pressures in particle growth.

Cappa & Wilson (2012) have developed a Statistical Oxidation Model (SOM), which simulates gas-phase chemistry and calculates the thermodynamic properties of HOMs. It explicitly takes into account multi-generational oxidation and fragmentation processes and assumes equilibrium gas-to-particle partitioning. The TwO Moment Aerosol Sectional (TOMAS) model uses a sectional approach to track the number and mass moments of the particle size distribution and simulates nucleation, coagulation, condensation, and evaporation processes (Adams & Seinfeld, 2002). These approaches are combined in the SOM-TOMAS model, where TOMAS models the kinetic condensation and evaporation of all SOM-determined species for each TOMAS size section. SOM-TOMAS has been used to simulate SOA formation (Akherati et al., 2020; He et al., 2020). TOMAS can also be combined with VBS, and that approach is used to model particle formation, condensation and coagulation of organic compounds (Hodshire et al., 2018).

Shiraiwa et al. (2010) have developed a kinetic multi-layer model of aerosol surface and bulk chemistry (KM-SUB), which explicitly resolves all steps of mass transport and chemical reaction at the surface and in the bulk of aerosol particles. It includes adsorption and desorption, surface reactions and surface-bulk exchange as well as bulk diffusion and reaction. Using KM-SUB, Shiraiwa et al. (2012) built a kinetic multi-layer model for gas-particle interactions in aerosols and clouds (KM-GAP), which also includes heat flux, evaporation and condensation of semi-volatile species. KM-GAP treats explicitly all steps of mass transport and chemical reaction of semi-volatile species partitioning between gas phase, particle surface and particle bulk. It has been used as a link between laboratory observations and molecular dynamics simulations, confirming that the best estimate of the surface accommodation coefficient of water vapor on a water droplet is close to unity. However, when the phase state of SOA is not liquid but (semi-)solid, the accommodation coefficient might be far from unity. Thus the phase state of atmospheric particles is highly relevant for chemical transformation and aging. The KM-GAP model resolves the effects of surface and bulk mass transport in particles undergoing condensation and evaporation, providing insights into atmospheric aging and chemical transformations.

Roldin et al. (2014) have developed the Aerosol Dynamics, gas- and particle-phase chemistry model for laboratory CHAMber studies (ADCHAM), which models non-equilibrium secondary organic aerosol (SOA) formation, evaporation, and chemical transformation. ADCHAM contains an aerosol dynamic module to simulate nucleation, coagulation, condensation and dry deposition, a detailed particle-phase chemistry module to model chemical reactions such as oligomerization, a kinetic multilayer module to treat the mass transfer limited diffusion of compounds in the particle phase, and a detailed gas-phase chemistry module with the near explicit Master Chemical Mechanism (MCM) (Jenkin et al., 1997). ADCHAM has been used to simulate, for instance, evaporation of sulfuric acid from sulfate aerosol particles (Tsagkogeorgas et al., 2017) and contribution of biogenic volatile organic compounds to particle formation during photooxidation chamber experiments (Roldin et al., 2015). Roldin et al. (2011) have also developed a trajectory model for Aerosol Dynamics, gas and particle phase CHEMistry and radiative transfer (ADCHEM). The model has been used to study the role of HOMs in particle growth over the boreal forest (Öström et al., 2017). In addition, it has been combined with cluster distribution simulations to study aerosol–cloud–climate systems, which allows an explicit inclusion of AN formation based on first-principles cluster data in the chemical transport model instead of simple parametrizations (Roldin et al., 2019). The model was used to reproduce the observed NPF, HOM gas-phase composition and SOA formation over the boreal forest.

3.2.2. Top-down modeling challenges and opportunities

It is worth noting that models relying on bulk thermodynamics might not fully capture the behavior of AN. This has been confirmed through modeling as well as experiments. For instance, Chen et al. (2018a) showed that AN acidity is dependent on particle size and the small ANs are not fully neutralized as bulk thermodynamics would predict. Using thermodynamic modeling they found that acid–base chemistry is less efficient in AN than in bulk and that $\mathrm{p}K_\mathrm{a}$ values should be modified up to 3.5 units in order for modeled acid-to-base ratios to agree with experimental observations. There is, currently, no way to represent this size-resolved chemistry in models.

While volatility basis sets are commonly used as a simplified measure for saturation vapor pressures, it should be noted that large errors might arise due to specific molecular structures. Kurtén et al. (2016) used the conductor-like screening model for real solvents (COSMO-RS) (Klamt & Eckert, 2000; Eckert & Klamt, 2002), which combines quantum chemistry with statistical thermodynamics, to compute the saturation vapor pressures for terpene autoxidation products and compared the results with three different group-contribution methods. They found that group contribution methods are likely to underestimate the vapor pressures of HOMs when they have intermolecular hydrogen bonds, whereas COSMO-RS overpredicts the effect of hydrogen bonding and leads to the overestimation of vapor pressures. Krieger et al. (2018) confirmed that COSMO-RS leads to overestimated vapor pressures compared to a validated set of measured vapor pressures for a homologous series of polyethylene glycols. By performing exhaustive conformational sampling and selecting only conformers with a minimum number of intermolecular hydrogen bonds, Kurtén et al. (2018) showed that computed vapor pressures can be substantially improved. COSMO-RS can also be used to predict other bulk properties of complex molecules in multicomponent mixtures, such as Setschenow constants, activity coefficients, and solubilities (Toivola et al., 2017; Hyttinen et al., 2020), but it should be kept in mind that the accuracy might not be sufficient for process-level models.

The treatment of gas phase chemistry in these models is important for determining precursors as well as for identifying possible particle-phase reactions. Many models use MCM, but applying more sophisticated models that more accurately predict HOM formation is necessary. Particle phase reactions such as acid–base chemistry and accretion reactions are acknowledged but it is not clear what the relative importance of these reactive uptake mechanisms is compared to reversible condensation of HOMs. Clearly, advances in understanding of both gas- and particle-phase chemistry will greatly benefit efforts to accurately model atmospheric AN formation.

4. Closing the gap between clusters and nanoparticles

As this review has shown, significant challenges exist, both in measurements and modeling, in understanding size-resolved composition of atmospheric aerosol nanoclusters. We close this review with a brief discussion of some of the most promising future directions that may lead to closing this gap.

With regards to measurements, opportunities already exist to close the 2–10 nm measurement gap by applying online, indirect approaches such as V/HTDMA and CPC batteries. While these measurements do not provide specific information on AN composition, their ability to provide insights into the chemical properties of ambient AN is unique among current approaches; such measurements are likely to be improved by recent advances in AN sizing and detection, making measurements in remote regions as well as aloft possible.

Online, direct measurements from the bottom-up have the potential to detect clusters larger than 2 nm through the application of mass spectrometers with extended mass range, but the cubic relationship of mass on diameter suggests that only minor gains in closing the gap are possible by such approaches. Mobility separation combined with mass spectrometry can potentially play a role in bridging the measurement gap. Since direct mass spectrometric detection over the diameter range of 2–10 nm is not possible, a means must be found to dissociate mobility-separated AN into constituent species that can be detected by mass spectrometry. There have been few attempts to perform mobility-based separation combined with ion dissociation using a traditional IMS-MS implementation (e.g., Krechmer et al. (2016)), but opportunities exist. For example, one could imagine an inlet in which high temperatures are applied to thermally decompose mobility-separated aerosol nanoclusters, after which an ionization method (e.g. chemical ionization or electron impact ionization) is applied to the products to enable mass spectrometric detection. Elements of this approach already exist, e.g. in an aerosol CIMS developed by Hearn & Smith (2004) and an IMS-MS with a secondary electrospray ionization source developed by Crawford et al. (2011).

Top-down approaches that combine mobility separation with nanoparticle dissociation followed by ionization and mass spectrometry possess a key advantage that makes the extension of their minimum detectable size into the AN size-range possible. Particle sampling losses in the 2–10 nm diameter range are governed by diffusion but there is otherwise no theoretical lower size limit that prevents these instruments from sampling AN. If atmospheric conditions allow for long collection times, then it may be possible for an approach such as TD-CIMS to sample particles to 5 nm and below but it will require further efficiency improvements of inlets, ion sources, and mass spectrometers. The previously mentioned NanoCharger, which combines charge enhancement with an aerodynamic concentrator, has potential to dramatically improve sample delivery to instruments such as NAMS and TDCIMS but this an area requiring further attention from the community. Ideally the dissociation of AN into constituent compounds is both quantitative and descriptive, but in reality achieving both is a major challenge. In current top-down approaches, NAMS has addressed quantitativeness by sacrificing certain aspects of descriptiveness, i.e. by measuring elemental and not molecular composition. TDCIMS can be highly descriptive through its ability to detect certain compounds such as mono- and dicarboxylic acids as molecular ions (Smith & Rathbone, 2008), but quantitativeness can be difficult to achieve for all but the simplest systems due to matrix effects and limitations of chemical ionization. The ideal combination of quantitativeness and descriptiveness may not be accessible for top-down measurements, so a combination of approaches is likely necessary.

With regards to modeling, machine learning might be an important tool for selecting the best cluster combinations for detailed study. While group contribution methods have been used to predict thermodynamic properties of unknown compounds based on existing molecular data, they suffer from lack of data especially for multifunctional, extremely low volatility compounds that are key participants in AN formation. More work is needed in adding details of molecular structure and non-linear interactions in order to improve the predictive power of group contribution methods. Descriptors such as Many-Body Tensor Representation, Coulomb Matrix and molecular fingerprints, which are used in machine learning methods to represent molecular geometry, have been shown to predict quantum mechanical properties of small neutral molecules within chemical accuracy (Cereto-Massagué et al., 2015; Rupp et al., 2012; Larsen et al., 2017; Himanen et al., 2020). While these descriptors have not been widely adopted by the atmospheric AN community, they have been used for other chemical systems. Low et al. (2020) have studied the effect of descriptor choice in machine learning models for ionic liquid melting point prediction with a kernel ridge regression model. They found that the addition of quantum chemical properties such as orbital energy and charge density to structural descriptors increases the accuracy of surrogate models for melting point prediction compared to using the structural descriptors alone. A similar approach, where the kernel ridge regression model is used to predict vapor pressure, could possibly be applicable to atmospheric compounds, thus helping to sort multifunctional organic compounds based on their AN formation ability. Pihlajamäki et al. (2020) developed a distance-based machine learning method and applied it to create a realistic atomistic interaction potential to be used in Monte Carlo simulations of metallic nanoparticles. Machine learning methods, once trained to model the system reliably, can speed up the simulations by several orders of magnitude and make it possible to study larger systems. These methods should be adapted to simulations of atmospheric AN formation and properties.

Another possibility to extend bottom-up approaches could be application of the hybrid quantum mechanics/molecular mechanics (QM/MM) approach (Warshel & Levitt, 1976), which combines the accuracy of QM and the speed of MM. In this approach, however, the user must know which part of a particle is active, i.e. where bonds are forming and breaking, thus the approach is often not straightforward. The QM/MM approach is widely used in biological studies to predict the activity of an enzyme against antibiotic agents (Hirvonen et al., 2019) and to study proton transfer pathways in a redox-driven proton pump (Di Luca et al., 2017). One possible application to atmospheric AN could be a reactive uptake of an organic compound on a salt particle, if it can be assumed that only the closest species of a partitioned molecule react and the rest of the particle remains unreactive. The QM/MM approach allows studies for larger particles compared to traditional quantum chemistry methods and it would be a helpful tool to study particles up to several nanometers.

While this review demonstrates the many measurement and modeling challenges that exist for determining 2–10 nm atmospheric aerosol nanocluster composition, it also highlights opportunities for closing this gap. We have chosen to separately discuss measurement and modeling approaches to AN composition, but it is already apparent that collaborations between these two groups can lead to significant advances. Models have already informed instrument development that have led to improved sensitivity and specificity, e.g. in understanding ion decomposition inside mass spectrometers and ion detection sensitivity of chemical ionization reagents. Measurements provide insights into which of the thousands of precursor vapors are most relevant to AN formation, significantly reducing computational costs. Closer connections between those who make and deploy instruments with modelers will be essential in making measurements of atmospheric aerosol nanoclusters routine.

About this review

The article is an editor-invited review article. Editor-Invited review articles began in 2020 to commemorate the 50th anniversary of the Journal of Aerosol Science.

Acknowledgement

The authors acknowledges funding from the U.S. National Science Foundation under Grants AGS-1762098, CHE-1710580, and CHE-2004066, and from the U.S. Department of Energy under Grant DE-SC0019000.

References

Adams, P. J., & Seinfeld, J. H. (2002). Predicting global aerosol size distributions in general circulation models. *Journal of Geophysical Research: Atmospheres*, *107*, AAC 4–1–AAC 4–23. URL: `https://agupubs.onlinelibrary.wiley.com/doi/abs/10.1029/2001JD001010`. doi:`10.1029/2001JD001010`.

Ahlm, L., Yli-Juuti, T., Schobesberger, S., Praplan, A. P., Kim, J., Tikkanen, O.-P., Lawler, M. J., Smith, J. N., Tröstl, J., Navarro, J. C. A., Baltensperger, U., Bianchi, F., Donahue, N. M., Duplissy, J., Franchin, A., Jokinen, T., Keskinen, H., Kirkby, J., Kürten, A., Laaksonen, A., Lehtipalo, K., Petäjä, T., Riccobono, F., Rissanen, M. P., Rondo, L., Schallhart, S., Simon, M., Winkler, P. M., Worsnop, D. R., Virtanen, A., & Riipinen, I. (2016). Modeling the thermodynamics and kinetics of sulfuric acid-dimethylamine-water nanoparticle growth in the cloud chamber. *Aerosol Science and Technology*, *50*, 1017–1032. doi:`10.1080/02786826.2016.1223268`.

Ahonen, L., Li, C., Kubečka, J., Iyer, S., Vehkamäki, H., Petäjä, T., Kulmala, M., & Hogan Jr, C. J. (2019). Ion mobility-mass spectrometry of iodine pentoxide–iodic acid hybrid cluster anions in dry and humidified atmospheres. *The Journal of Physical Chemistry Letters*, *10*, 1935–1941. URL: `https://doi.org/10.1021/acs.jpclett.9b00453`. doi:`10.1021/acs.jpclett.9b00453`. `arXiv:https://doi.org/10.1021/acs.jpclett.9b00453`.

Akherati, A., He, Y., Coggon, M. M., Koss, A. R., Hodshire, A. L., Sekimoto, K., Warneke, C., de Gouw, J., Yee, L., Seinfeld, J. H., Onasch, T. B., Herndon, S. C., Knighton, W. B., Cappa, C. D., Kleeman, M. J., Lim, C. Y., Kroll, J. H., Pierce, J. R., & Jathar, S. H. (2020). Oxygenated aromatic compounds are important precursors of secondary organic aerosol in biomass-burning emissions. *Environmental Science & Technology*, *54*, 8568–8579. doi:`10.1021/acs.est.0c01345`.

Allen, D. T., Palen, E. J., Haimov, M. I., Hering, S. V., & Young, J. R. (1994). Fourier Transform Infrared Spectroscopy of Aerosol Collected in a Low Pressure Impactor (LPI/FTIR): Method Development and Field Calibration. *Aerosol Science and Technology*, *21*, 325–342. URL: `https://doi.org/10.1080/02786829408959719`. doi:`10.1080/02786829408959719`.

Allinger, N. (1977). Conformational analysis. 130. mm2. a hydrocarbon force field utilizing v1 and v2 torsional terms. *J. Am. Chem. Soc.*, *99*, 8127–8134.

Angelino, S., Suess, D. T., & Prather, K. A. (2001). Formation of aerosol particles from reactions of secondary and tertiary alkylamines: Characterization by aerosol time-of-flight mass spectrometry. *Environ. Sci. Technol.*, *35*, 3130–3138.

Arffman, A., Yli-Ojanperä, J., Kalliokoski, J., Harra, J., Pirjola, L., Karjalainen, P., Rönkkö, T., & Keskinen, J. (2014). High-resolution low-pressure cascade impactor. *Journal of Aerosol Science*, *78*, 97–109. URL: `http://dx.doi.org/10.1016/j.jaerosci.2014.08.006`. doi:`10.1016/j.jaerosci.2014.08.006`.

Arquero, K. D., Xu, J., Gerber, R. B., & Finlayson-Pitts, B. J. (2017). Particle formation and growth from oxalic acid, methanesulfonic acid, trimethylamine and water: a combined experimental and theoretical study. *Physical Chemistry Chemical Physics*, *19*, 28286–28301.

Barsanti, K. C., & Pankow, J. F. (2004). Thermodynamics of the formation of atmospheric organic particulate matter by accretion reactions—part 1: Aldehydes and ketones. *Atmos. Environ.*, *38*, 4371–4382.

Barsanti, K. C., & Pankow, J. F. (2005). Thermodynamics of the formation of atmospheric organic particulate matter by accretion reactions—2. dialdehydes, methylglyoxal, and diketones. *Atmos. Environ.*, *39*, 6597–6607.

Barsanti, K. C., & Pankow, J. F. (2006). Thermodynamics of the formation of atmospheric organic particulate matter by accretion reactions—part 3: Carboxylic and dicarboxylic acids. *Atmos. Environ.*, *40*, 6676–6686.

Bertram, T. H., Kimmel, J. R., Crisp, T. A., Ryder, O. S., Yatavelli, R. L. N., Thornton, J. A., Cubison, M. J., Gonin, M., & Worsnop, D. R. (2011). A field-deployable, chemical ionization time-of-flight mass spectrometer. *Atmospheric Measurement Techniques*, *4*, 1471–1479. URL: `https://amt.copernicus.org/articles/4/1471/2011/`. doi:`10.5194/amt-4-1471-2011`.

Besel, V., Kubečka, J., Kurtén, T., & Vehkamäki, H. (2020). Impact of quantum chemistry parameter choices and cluster distribution model settings on modeled atmospheric particle formation rates. *The Journal of Physical Chemistry A*, *124*, 5931–5943. doi:`10.1021/acs.jpca.0c03984`.

Bianchi, F., Kurtén, T., Riva, M., Mohr, C., Rissanen, M. P., Roldin, P., Berndt, T., Crounse, J. D., Wennberg, P. O., Mentel, T. F., Wildt, J., Junninen, H., Jokinen, T., Kulmala, M., Worsnop, D. R., Thornton, J. A., Donahue, N., Kjaergaard, H. G., & Ehn, M. (2019). Highly oxygenated organic molecules (hom) from gas-phase autoxidation involving peroxy radicals: A key contributor to atmospheric aerosol. *Chemical Reviews*, *119*, 3472–3509. doi:`10.1021/acs.chemrev.8b00395`.

Bianchi, F., Tröstl, J., Junninen, H., Frege, C., Henne, S., Hoyle, C. R., Molteni, U., Herrmann, E., Adamov, A., Bukowiecki, N., Chen, X., Duplissy, J., Gysel, M., Hutterli, M., Kangasluoma, J., Kontkanen, J., Kürten, A., Manninen, H. E., Münch, S., Peräkylä, O., Petäjä, T., Rondo, L., Williamson, C., Weingartner, E., Curtius, J., Worsnop, D. R., Kulmala, M., Dommen, J., & Baltensperger, U. (2016). New particle formation in the free troposphere: A question of chemistry and timing. *Science*, *352*, 1109–1112. URL: `http://science.sciencemag.org/content/early/2016/05/24/science.aad5456.abstract`. doi:`10.1126/science.aad5456`.

Bzdek, B. R., Lawler, M. J., Horan, A. J., Pennington, M. R., DePalma, J. W., Zhao, J., Smith, J. N., & Johnston, M. V. (2014). Molecular constraints on particle growth during new particle formation. *Geophysical Research Letters*, *41*, 6045–6054. doi:`10.1002/2014GL060160`.

Bzdek, B. R., Ridge, D. P., & Johnston, M. V. (2010a). Amine exchange into ammonium bisulfate and ammonium nitrate nuclei. *Atmos. Chem. Phys.*, *10*, 3495–3503. URL: `https://www.atmos-chem-phys.net/10/3495/2010/`. doi:`10.5194/acp-10-3495-2010`.

Bzdek, B. R., Ridge, D. P., & Johnston, M. V. (2010b). Size-dependent reactions of ammonium bisulfate clusters with dimethylamine. *J. Phys. Chem. A*, *114*, 11638–11644. doi:`10.1021/jp106363m`.

Bzdek, B. R., Zordan, C. A., Pennington, M. R., Luther, G. W., & Johnston, M. V. (2012). Quantitative assessment of the sulfuric acid contribution to new particle growth. *Environmental Science and Technology*, *46*, 4365–4373. doi:`10.1021/es204556c`.

Canagaratna, M. R., Jayne, J. T., Jimenez, J. L., Allan, J. D., Alfarra, M. R., Zhang, Q., Onasch, T. B., Drewnick, F., Coe, H., Middlebrook, A., Delia, A., Williams, L. R., Trimborn, A. M., Northway, M. J., DeCarlo, P. F., Kolb, C. E., Davidovits, P., & Worsnop, D. R. (2007). Chemical and microphysical characterization of ambient aerosols with the aerodyne aerosol mass spectrometer. *Mass Spectrometry Reviews*, *26*, 185–222. doi:`10.1002/mas.20115`.

Cappa, C. D., & Wilson, K. R. (2012). Multi-generation gas-phase oxidation, equilibrium partitioning, and the formation and evolution of secondary organic aerosol. *Atmospheric Chemistry and Physics*, *12*, 9505–9528. doi:`10.5194/acp-12-9505-2012`.

Car, R., & Parrinello, M. (1985). Unified approach for molecular dynamics and density-functional theory. *Phys. Rev. Lett.*, *55*, 2471.

Cereto-Massagué, A., Ojeda, M. J., Valls, C., Mulero, M., Garcia-Vallvé, S., & Pujadas, G. (2015). Molecular fingerprint similarity search in virtual screening. *Methods*, *71*, 58 – 63. URL: `http://www.sciencedirect.com/science/article/pii/S1046202314002631`. doi:`https://doi.org/10.1016/j.ymeth.2014.08.005`. Virtual Screening.

Chee, S., Myllys, N., Barsanti, K. C., Wong, B. M., & Smith, J. N. (2019). An experimental and modeling study of nanoparticle formation and growth from dimethylamine and nitric acid. *J. Phys. Chem. A*, *123*, 5640–5648. doi:`10.1021/acs.jpca.9b03326`.

Chen, H., Chee, S., Lawler, M. J., Barsanti, K. C., Wong, B. M., & Smith, J. N. (2018a). Size resolved chemical composition of nanoparticles from reactions of sulfuric acid with ammonia and dimethylamine. *Aerosol Science and Technology*, *52*, 1120–1133. URL: `https://doi.org/10.1080/02786826.2018.1490005`. doi:`10.1080/02786826.2018.1490005`.

Chen, H., Hodshire, A. L., Ortega, J., Greenberg, J., McMurry, P. H., Carlton, A. G., Pierce, J. R., Hanson, D. R., & Smith, J. N. (2018b). Vertically resolved concentration and liquid water content of atmospheric nanoparticles at the US DOE Southern Great Plains site. *Atmospheric Chemistry and Physics*, *18*, 311–326. URL: `https://www.atmos-chem-phys-discuss.net/acp-2017-586/`. doi:`10.5194/acp-18-311-2018`.

Chen, M., Titcombe, M., Jiang, J., Jen, C., Kuang, C., Fischer, M. L., Eisele, F. L., Siepmann, J. I., Hanson, D. R., Zhao, J., & McMurry, P. H. (2012). Acid-base chemical reaction model for nucleation rates in the polluted atmospheric boundary layer. *Proceedings of the National Academy of Sciences of the United States of America*, *109*, 18713–18718. URL: `http://www.pnas.org/content/early/2012/10/17/1210285109.abstract`. doi:`10.1073/pnas.1210285109`.

Chen, X., Jiang, J., & Chen, D. R. (2019). Maximizing the singly charged fraction of sub-micrometer particles using a unipolar charger. *Aerosol Science and Technology*, *53*, 990–997. URL: `https://doi.org/10.1080/02786826.2019.1617833`. doi:`10.1080/02786826.2019.1617833`.

Clegg, S. L., Pitzer, K. S., & Brimblecombe, P. (1992). Thermodynamics of multicomponent, miscible, ionic solutions. mixtures including unsymmetrical electrolytes. *The Journal of Physical Chemistry*, *96*, 9470–9479. doi:`10.1021/j100202a074`.

Crawford, C. L., Graf, S., Gonin, M., Fuhrer, K., Zhang, X., & Hill, H. H. (2011). The novel use of gas chromatography-ion mobility-time of flight mass spectrometry with secondary electrospray ionization for complex mixture analysis. *International Journal for Ion Mobility Spectrometry*, *14*, 23–30. URL: `https://doi.org/10.1007/s12127-010-0057-2`. doi:`10.1007/s12127-010-0057-2`.

Day, P. N., Pachter, R., Gordon, M. S., & Merrill, G. N. (2000). A study of water clusters using the effective fragment potential and monte carlo simulated annealing. *The Journal of Chemical Physics*, *112*, 2063–2073.

DePalma, J. W., Bzdek, B. R., Ridge, D. P., & Johnston, M. V. (2014a). Activation barriers in the growth of molecular clusters derived from sulfuric acid and ammonia. *The Journal of Physical Chemistry A*, *118*, 11547–11554. doi:`10.1021/jp507769b`.

DePalma, J. W., Doren, D. J., & Johnston, M. V. (2014b). Formation and growth of molecular clusters containing sulfuric acid, water, ammonia, and dimethylamine. *J. Phys. Chem. A*, *118*, 5464–5473.

Di Luca, A., Gamiz-Hernandez, A. P., & Kaila, V. R. I. (2017). Symmetry-related proton transfer pathways in respiratory complex i. *Proceedings of the National Academy of Sciences*, *114*, E6314–E6321. URL: `https://www.pnas.org/content/114/31/E6314`. doi:`10.1073/pnas.1706278114`. `arXiv:https://www.pnas.org/content/114/31/E6314.full.pdf`.

Donahue, N. M., Epstein, S. A., Pandis, S. N., & Robinson, A. L. (2011). A two-dimensional volatility basis set: 1. organic-aerosol mixing thermodynamics. *Atmospheric Chemistry and Physics*, *11*, 3303–3318. URL: `https://www.atmos-chem-phys.net/11/3303/2011/`. doi:`10.5194/acp-11-3303-2011`.

Donahue, N. M., Kroll, J. H., Pandis, S. N., & Robinson, A. L. (2012). A two-dimensional volatility basis set – part 2: Diagnostics of organic-aerosol evolution. *Atmospheric Chemistry and Physics*, *12*, 615–634. URL: `https://www.atmos-chem-phys.net/12/615/2012/`. doi:`10.5194/acp-12-615-2012`.

Draper, D. C., Myllys, N., Hyttinen, N., Møller, K. H., Kjaergaard, H. G., Fry, J. L., Smith, J. N., & Kurtén, T. (2019). Formation of highly oxidized molecules from no3 radical initiated oxidation of Δ-3-carene: A mechanistic study. *ACS Earth and Space Chemistry*, *3*, 1460–1470. doi:`10.1021/acsearthspacechem.9b00143`.

Eckert, F., & Klamt, A. (2002). Fast solvent screening via quantum chemistry: Cosmo-rs approach. *AIChE Journal*, *48*, 369–385.

Eisele, F. L. (1989). Natural and anthropogenic negative ions in the troposphere. *Journal of Geophysical Research: Atmospheres*, *94*, 2183–2196. URL: `https://agupubs.onlinelibrary.wiley.com/doi/abs/10.1029/JD094iD02p02183`. doi:`10.1029/JD094iD02p02183`. `arXiv:https://agupubs.onlinelibrary.wiley.com/doi/pdf/10.1029/JD094iD02p02183`.

Eisele, F. L., Lovejoy, E. R., Kosciuch, E., Moore, K. F., Mauldin III, R. L., Smith, J. N., McMurry, P. H., & Iida, K. (2006). Negative atmospheric ions and their potential role in ion-induced nucleation. *Journal of Geophysical Research: Atmospheres*, *111*. URL: `https://agupubs.onlinelibrary.wiley.com/doi/abs/10.1029/2005JD006568`. doi:`10.1029/2005JD006568`. `arXiv:https://agupubs.onlinelibrary.wiley.com/doi/pdf/10.1029/2005JD006568`.

Eisele, F. L., & Tanner, D. J. (1993). Measurement of the gas phase concentration of H2SO4 and methane sulfonic acid and estimates of H2SO4 production and loss in the atmosphere. *Journal of Geophysical Research*, *98*, 9001–9010. doi:`10.1029/93JD00031`.

Elm, J. (2019). Unexpected growth coordinate in large clusters consisting of sulfuric acid and c8h12o6 tricarboxylic acid. *The Journal of Physical Chemistry A*, *123*, 3170–3175. doi:`10.1021/acs.jpca.9b00428`.

Elm, J., Bilde, M., & Mikkelsen, K. V. (2012). Assessment of density functional theory in predicting structures and free energies of reaction of atmospheric prenucleation clusters. *J. Chem. Theory Comput.*, *8*, 2071–2077. doi:`10.1021/ct300192p`.

Elm, J., & Kristensen, K. (2017). Basis set convergence of the binding energies of strongly hydrogen-bonded atmospheric clusters. *Phys. Chem. Chem. Phys.*, *19*, 1122–1133. URL: `http://dx.doi.org/10.1039/C6CP06851K`. doi:`10.1039/C6CP06851K`.

Elm, J., Kubečka, J., Besel, V., Jääskeläinen, M. J., Halonen, R., Kurtén, T., & Vehkamäki, H. (2020). Modeling the formation and growth of atmospheric molecular clusters: A review. *Journal of Aerosol Science*, *149*, 105621. URL: `http://www.sciencedirect.com/science/article/pii/S0021850220301099`. doi:`https://doi.org/10.1016/j.jaerosci.2020.105621`.

Elm, J., & Mikkelsen, K. V. (2014). Computational approaches for efficiently modelling of small atmospheric clusters. *Chem. Phys. Lett.*, *615*, 26–29. URL: `http://www.sciencedirect.com/science/article/pii/S0009261414008379`. doi:`http://dx.doi.org/10.1016/j.cplett.2014.09.060`.

Elm, J., Myllys, N., Hyttinen, N., & Kurtén, T. (2015). Computational study of the clustering of a cyclohexene autoxidation product $C_6H_8O_7$ with itself and sulfuric acid. *J. Phys. Chem. A*, *119*, 8414–8421. doi:`10.1021/acs.jpca.5b04040`.

Elm, J., Myllys, N., & Kurtén, T. (2017a). Phosphoric acid–a potentially elusive participant in atmospheric new particle formation. *Molecular Physics*, *115*, 2168–2179.

Elm, J., Myllys, N., & Kurtén, T. (2017b). What is required for highly oxidized molecules to form clusters with sulfuric acid? *J. Phys. Chem. A*, *121*, 4578–4587. doi:`10.1021/acs.jpca.7b03759`.

Elm, J., Myllys, N., Luy, J.-N., Kurtén, T., & Vehkamäki, H. (2016). The effect of water and bases on the clustering of a cyclohexene autoxidation product $C_6H_8O_7$ with sulfuric acid. *J. Phys. Chem. A*, *120*, 2240–2249. doi:`10.1021/acs.jpca.6b00677`.

Elm, J., Myllys, N., Olenius, T., Halonen, R., Kurtén, T., & Vehkämaki, H. (2017c). Formation of atmospheric molecular clusters consisting of sulfuric acid and $C_8H_{12}O_6$ tricarboxylic acid. *Phys. Chem. Chem. Phys.*, *19*, 4877–4886. URL: `http://dx.doi.org/10.1039/C6CP08127D`. doi:`10.1039/C6CP08127D`.

Erickson, H. P. (2009). Size and shape of protein molecules at the nanometer level determined by sedimentation, gel filtration, and electron microscopy. *Biological procedures online*, *11*, 32–51. URL: `https://pubmed.ncbi.nlm.nih.gov/19495910https://www.ncbi.nlm.nih.gov/pmc/articles/PMC3055910/`. doi:`10.1007/s12575-009-9008-x`.

Fialkov, A. B., Steiner, U., Lehotay, S. J., & Amirav, A. (2007). Sensitivity and noise in GC–MS: Achieving low limits of detection for difficult analytes. *International Journal of Mass Spectrometry*, *260*, 31–48. URL: `http://www.sciencedirect.com/science/article/pii/S1387380606003423`. doi:`https://doi.org/10.1016/j.ijms.2006.07.002`.

Gale, A. G., Odbadrakh, T. T., Ball, B. T., & Shields, G. C. (2020). Water-mediated peptide bond formation in the gas phase: A model prebiotic reaction. *The Journal of Physical Chemistry A*, *124*, 4150–4159. doi:`10.1021/acs.jpca.0c02906`.

Gard, E., Mayer, J. E., Morrical, B. D., Dienes, T., Fergenson, D. P., & Prather, K. A. (1997). Real-Time Analysis of Individual Atmospheric Aerosol Particles: Design and Performance of a Portable ATOFMS. *Analytical Chemistry*, *69*, 4083–4091. doi:`10.1021/ac970540n`.

Geller, M. D., Biswas, S., Fine, P. M., & Sioutas, C. (2005). A new compact aerosol concentrator for use in conjunction with low flow-rate continuous aerosol instrumentation. *Journal of Aerosol Science*, *36*, 1006–1022. URL: `http://www.sciencedirect.com/science/article/pii/S0021850204004082`. doi:`https://doi.org/10.1016/j.jaerosci.2004.11.015`.

Geller, M. D., Kim, S., Misra, C., Sioutas, C., Olson, B. A., & Marple, V. A. (2002). A methodology for measuring size-dependent chemical composition of ultrafine particles. *Aerosol Science and Technology*, *36*, 748–762. doi:`10.1080/02786820290038447`.

Glasoe, W. A., Volz, K., Panta, B., Freshour, N., Bachman, R., Hanson, D. R., McMurry, P. H., & Jen, C. (2015). Sulfuric acid nucleation: An experimental study of the effect of seven bases. *J. Geophys. Res. Atmos.*, *120*, 1933–1950. URL: `https://agupubs.onlinelibrary.wiley.com/doi/abs/10.1002/2014JD022730`. doi:`10.1002/2014JD022730`.

Gonser, S. G., & Held, A. (2013). A chemical analyzer for charged ultrafine particles. *Atmospheric Measurement Techniques*, *6*, 2339–2348. URL: `https://amt.copernicus.org/articles/6/2339/2013/`. doi:`10.5194/amt-6-2339-2013`.

González, Á. (2010). Measurement of areas on a sphere using fibonacci and latitude–longitude lattices. *Mathematical Geosciences*, *42*, 49.

Grimme, S. (2012). Supramolecular binding thermodynamics by dispersion-corrected density functional theory. *Chemistry–A European Journal*, *18*, 9955–9964.

Halonen, R., Zapadinsky, E., Kurtén, T., Vehkamäki, H., & Reischl, B. (2019). Rate enhancement in collisions of sulfuric acid molecules due to long-range intermolecular forces. *Atmospheric Chemistry and Physics*, *19*, 13355–13366.

Hartke, B., Schütz, M., & Werner, H.-J. (1998). Improved intermolecular water potential from global geometry optimization of small water clusters using local mp2. *Chemical physics*, *239*, 561–572.

He, S., Li, L., Duan, H., Naqwi, A., & Hogan, C. J. (2015). Aerosol Analysis via Electrostatic Precipitation-Electrospray Ionization Mass Spectrometry. *Analytical Chemistry*, *87*, 6752–6760. doi:`10.1021/acs.analchem.5b01183`.

He, Y., King, B., Pothier, M., Lewane, L., Akherati, A., Mattila, J., Farmer, D. K., McCormick, R. L., Thornton, M., Pierce, J. R., Volckens, J., & Jathar, S. H. (2020). Secondary organic aerosol formation from evaporated biofuels: comparison to gasoline and correction for vapor wall losses. *Envi-*

ron. Sci.: Processes Impacts, *22*, 1461–1474. URL: `http://dx.doi.org/10.1039/D0EM00103A`. doi:`10.1039/D0EM00103A`.

Hearn, J. D., & Smith, G. D. (2004). A Chemical Ionization Mass Spectrometry Method for the Online Analysis of Organic Aerosols. *Analytical Chemistry*, *76*, 2820–2826. URL: `https://doi.org/10.1021/ac049948s`. doi:`10.1021/ac049948s`.

Henschel, H., Kurtén, T., & Vehkamäki, H. (2016). Computational study on the effect of hydration on new particle formation in the sulfuric acid/ammonia and sulfuric acid/dimethylamine systems. *J. Phys. Chem. A*, *120*, 1886–1896. doi:`10.1021/acs.jpca.5b11366`.

Hering, S. V., & Stolzenburg, M. R. (2005). A method for particle size amplification by water condensation in a laminar, thermally diffusive flow. *Aerosol Science and Technology*, *39*, 428–436. doi:`10.1080/027868290953416`.

Himanen, L., Jäger, M. O., Morooka, E. V., Federici Canova, F., Ranawat, Y. S., Gao, D. Z., Rinke, P., & Foster, A. S. (2020). Dscribe: Library of descriptors for machine learning in materials science. *Computer Physics Communications*, *247*, 106949. URL: `http://www.sciencedirect.com/science/article/pii/S0010465519303042`. doi:`https://doi.org/10.1016/j.cpc.2019.106949`.

Hirvonen, V., Myllys, N., Kurtén, T., & Elm, J. (2018). Closed-shell organic compounds might form dimers at the surface of molecular clusters. *J. Phys. Chem. A*, *122*, 1771–1780. doi:`10.1021/acs.jpca.7b11970`.

Hirvonen, V. H. A., Hammond, K., Chudyk, E. I., Limb, M. A. L., Spencer, J., Mulholland, A. J., & van der Kamp, M. W. (2019). An efficient computational assay for B-lactam antibiotic breakdown by class a B-lactamases. *Journal of Chemical Information and Modeling*, *59*, 3365–3369. doi:`10.1021/acs.jcim.9b00442`.

Hodshire, A. L., Palm, B. B., Alexander, M. L., Bian, Q., Campuzano-Jost, P., Cross, E. S., Day, D. A., de Sá, S. S., Guenther, A. B., Hansel, A., Hunter, J. F., Jud, W., Karl, T., Kim, S., Kroll, J. H., Park, J.-H., Peng, Z., Seco, R., Smith, J. N., Jimenez, J. L., & Pierce, J. R. (2018). Constraining nucleation, condensation, and chemistry in oxidation flow reactors using size-distribution measurements and aerosol microphysical modeling. *Atmospheric Chemistry and Physics*, *18*, 12433–12460. URL: `https://www.atmos-chem-phys.net/18/12433/2018/`. doi:`10.5194/acp-18-12433-2018`.

Horan, A. J., Apsokardu, M. J., & Johnston, M. V. (2017a). Droplet assisted inlet ionization for online analysis of airborne nanoparticles. *Analytical Chemistry*, *89*, 1059–1062. doi:`10.1021/acs.analchem.6b04718`.

Horan, A. J., Krasnomowitz, J. M., & Johnston, M. V. (2017b). Particle size and chemical composition effects on elemental analysis with the nano aerosol mass spectrometer. *Aerosol Science and Technology*, *51*, 1135–1143. URL: `https://doi.org/10.1080/02786826.2017.1335390`. doi:`10.1080/02786826.2017.1335390`.

Hu, R., Zhang, L., & Yang, Z. (2007). Picogram determination of estrogens in water using large volume injection gas chromatography–mass spectrometry. *Analytical and Bioanalytical Chemistry*, *390*, 349. URL: `https://doi.org/10.1007/s00216-007-1683-3`. doi:`10.1007/s00216-007-1683-3`.

Hyttinen, N., Elm, J., Malila, J., Calderón, S. M., & Prisle, N. L. (2020). Thermodynamic properties of isoprene- and monoterpene-derived organosulfates estimated with cosmo*therm*. *Atmospheric Chemistry and Physics*, *20*, 5679–5696. URL: `https://acp.copernicus.org/articles/20/5679/2020/`. doi:`10.5194/acp-20-5679-2020`.

Hyttinen, N., Otkjær, R. V., Iyer, S., Kjaergaard, H. G., Rissanen, M. P., Wennberg, P. O., & Kurtén, T. (2018). Computational comparison of different reagent ions in the chemical ionization of oxidized multifunctional compounds. *The Journal of Physical Chemistry A*, *122*, 269–279.

Iyer, S., Lopez-Hilfiker, F., Lee, B. H., Thornton, J. A., & Kurtén, T. (2016). Modeling the detection of organic and inorganic compounds using iodide-based chemical ionization. *The Journal of Physical Chemistry A*, *120*, 576–587. doi:`10.1021/acs.jpca.5b09837`.

Jenkin, M. E., Saunders, S. M., & Pilling, M. J. (1997). The tropospheric degradation of volatile organic compounds: a protocol for mechanism development. *Atmospheric environment*, *31*, 81–104.

Jokinen, T., Sipilä, M., Junninen, H., Ehn, M., Lönn, G., Hakala, J., Petäjä, T., Mauldin, R. L., Kulmala, M., & Worsnop, D. R. (2012). Atmospheric sulphuric acid and neutral cluster measurements using CI-APi-TOF. *Atmospheric Chemistry and Physics*, *12*, 4117–4125. URL: `http://www.atmos-chem-phys.net/12/4117/2012/http://www.atmos-chem-phys.net/12/4117/2012/acp-12-4117-2012.pdf`. doi:`10.5194/acp-12-4117-2012`.

Joutsensaari, J., Vaattovaara, P., Vesterinen, M., Hämeri, K., & Laaksonen, A. (2001). A novel tandem differential mobility analyzer with organic vapor treatment of aerosol particles. *Atmospheric Chemistry and Physics*, *1*, 51–60. URL: `http://www.atmos-chem-phys.net/1/51/2001/`. doi:`10.5194/acp-1-51-2001`.

Junninen, H., Ehn, M., Petäjä, Luosujärvi, L., Kotiaho, T., Kostiainen, R., Rohner, U., Gonin, M., Fuhrer, K., Kulmala, M., & Worsnop, D. R. (2010). A high-resolution mass spectrometer to measure atmospheric ion composition. *Atmospheric Measurement Techniques*, *3*, 1039–1053. URL: `http://www.atmos-meas-tech.net/3/1039/2010/http://www.atmos-meas-tech.net/3/1039/2010/amt-3-1039-2010.pdf`. doi:`10.5194/amt-3-1039-2010`.

Kalberer, M., Morrical, B. D., Sax, M., & Zenobi, R. (2002). Picogram Quantitation of Polycyclic Aromatic Hydrocarbons Adsorbed on Aerosol Particles by Two-Step Laser Mass Spectrometry. *Analytical Chemistry*, *74*, 3492–3497. URL: `https://doi.org/10.1021/ac011233r`. doi:`10.1021/ac011233r`.

Kangasluoma, J., Cai, R., Jiang, J., Deng, C., Stolzenburg, D., Ahonen, L. R., Chan, T., Fu, Y., Kim, C., Laurila, T. M., Zhou, Y., Dada, L., Sulo, J., Flagan, R. C., Kulmala, M., Petäjä, T., & Lehtipalo, K. (2020). Overview of measurements and current instrumentation for 1–10 nm aerosol particle number size distributions. *Journal of Aerosol Science*, *148*, 105584. URL: `http://www.sciencedirect.com/science/article/pii/S0021850220300732`. doi:`10.1016/j.jaerosci.2020.105584`.

Kerminen, V. M. (1997). The effects of particle chemical character and atmospheric processes on particle hygroscopic properties. *Journal of Aerosol Science*, *28*, 121–132. doi:`10.1016/S0021-8502(96)00069-9`.

Kerminen, V.-M., Chen, X., Vakkari, V., Petäjä, T., Kulmala, M., & Bianchi, F. (2018). Atmospheric new particle formation and growth: review of field observations. *Environmental Research Letters*, *13*, 103003. URL: `http://dx.doi.org/10.1088/1748-9326/aadf3c`. doi:`10.1088/1748-9326/aadf3c`.

Kildgaard, J. V., Mikkelsen, K. V., Bilde, M., & Elm, J. (2018a). Hydration of atmospheric molecular clusters: A new method for systematic configurational sampling. *The Journal of Physical Chemistry A*, *122*, 5026–5036. doi:`10.1021/acs.jpca.8b02758`.

Kildgaard, J. V., Mikkelsen, K. V., Bilde, M., & Elm, J. (2018b). Hydration of atmospheric molecular clusters ii: Organic acid–water clusters. *The Journal of Physical Chemistry A*, *122*, 8549–8556.

Kirkby, J., Duplissy, J., Sengupta, K., Frege, C., Gordon, H., Williamson, C., Heinritzi, M., Simon, M., Yan, C., Almeida, J., Trostl, J., Nieminen, T., Ortega, I., Wagner, R., Adamov, A., Amorim, A., Bernhammer, A.-K., Bianchi, F., Breitenlechner, M., Brilke, S., Chen, X., Craven, J., Dias, A., Ehrhart, S., Flagan, R., Franchin, A., Fuchs, C., Guida, R., Hakala, J., Hoyle, C., Jokinen, T., Junninen, H., Kangasluoma, J., Kim, J., Krapf, M., Kurtén, A., Laaksonen, A., Lehtipalo, K., Makhmutov, V., Mathot, S., Molteni, U., Onnela, A., Perakyla, O., Piel, F., Petaja, T., Praplan, A., Pringle, K., Rap, A., Richards, N., Riipinen, I., Rissanen, M., Rondo, L., Sarnela, N., Schobesberger, S., Scott, C., Seinfeld, J., Sipilä, M., Steiner, G., Stozhkov, Y., Stratmann, F., TomÃ©, A., Virtanen, A., Vogel, A., Wagner, A., Wagner, P., Weingartner, E., Wimmer, D., Winkler, P., Ye, P., Zhang, X., Hansel, A., Dommen, J., Donahue, N., Worsnop, D., Baltensperger, U., Kulmala, M., Carslaw, K., & Curtius, J. (2016). Ion-induced nucleation of pure biogenic particles. *Nature*, *533*, 521–526. doi:`10.1038/nature17953`.

Kirkpatrick, S., Gelatt, C. D., & Vecchi, M. P. (1983). Optimization by simulated annealing. *science*, *220*, 671–680.

Klamt, A., & Eckert, F. (2000). Cosmo-rs: a novel and efficient method for the a priori prediction of thermophysical data of liquids. *Fluid Phase Equilibria*, *172*, 43–72.

Krechmer, J. E., Groessl, M., Zhang, X., Junninen, H., Massoli, P., Lambe, A. T., Kimmel, J. R., Cubison, M. J., Graf, S., Lin, Y.-H., Budisulistiorini, S. H., Zhang, H., Surratt, J. D., Knochenmuss, R., Jayne, J. T., Worsnop, D. R., Jimenez, J.-L., & Canagaratna, M. R. (2016). Ion mobility spectrometry–mass spectrometry (ims–ms) for on- and offline analysis of atmospheric gas and aerosol species. *Atmospheric Measurement Techniques*, *9*, 3245–3262. URL: `https://amt.copernicus.org/articles/9/3245/2016/`. doi:`10.5194/amt-9-3245-2016`.

Kreisberg, N. M., Spielman, S. R., Eiguren-Fernandez, A., Hering, S. V., Lawler, M. J., Draper, D. C., & Smith, J. N. (2018). Water condensation-based nanoparticle charging system: Physical and chemical characterization. *Aerosol Science and Technology*, *52*, 1167–1177. doi:`10.1080/02786826.2018.1503640`.

Krieger, U. K., Siegrist, F., Marcolli, C., Emanuelsson, E. U., Gøbel, F. M., Bilde, M., Marsh, A., Reid, J. P., Huisman, A. J., Riipinen, I., Hyttinen, N., Myllys, N., Kurtén, T., Bannan, T., Percival, C. J., & Topping, D. (2018). A reference data set for validating vapor pressure measurement techniques: homologous series of polyethylene glycols. *Atmospheric Measurement Techniques*, *11*, 49–63. URL: `https://amt.copernicus.org/articles/11/49/2018/`. doi:`10.5194/amt-11-49-2018`.

Kroll, J. H., Donahue, N. M., Jimenez, J. L., Kessler, S. H., Canagaratna, M. R., Wilson, K. R., Altieri, K. E., Mazzoleni, L. R., Wozniak, A. S., Bluhm, H. et al. (2011). Carbon oxidation state as a metric for describing the chemistry of atmospheric organic aerosol. *Nature Chemistry*, *3*, 133–139.

Kuang, C., Chen, M., Zhao, J., Smith, J., McMurry, P. H., & Wang, J. (2011). First size-dependent growth rate measurements of 1 to 5 nm freshly formed atmospheric nuclei. *Atmospheric Chemistry and Physics Discussions*, *11*, 25427–25471. URL: `http://www.atmos-chem-phys-discuss.net/11/25427/2011/`. doi:`10.5194/acpd-11-25427-2011`.

Kuang, C., Chen, M., Zhao, J., Smith, J., McMurry, P. H., & Wang, J. (2012). Size and time-resolved growth rate measurements of 1 to 5 nm freshly formed atmospheric nuclei. *Atmospheric Chemistry and Physics*, *12*, 3573–3589. URL: `http://10.0.20.74/acp-12-3573-2012http://www.atmos-chem-phys-discuss.net/11/25427/2011/`. doi:`10.5194/acp-12-3573-2012`.

Kuang, C., McMurry, P. H., & McCormick, A. V. (2009). Determination of cloud condensation nuclei production from measured new particle formation events. *Geophysical Research Letters*, *36*, n/a—-n/a. URL: `http://10.0.4.5/2009GL037584`. doi:`10.1029/2009GL037584`.

Kubečka, J., Besel, V., Kurtén, T., Myllys, N., & Vehkamäki, H. (2019). Configurational sampling of noncovalent (atmospheric) molecular clusters: Sulfuric acid and guanidine. *J. Phys. Chem. A*, *123*, 6022–6033. doi:`10.1021/acs.jpca.9b03853`.

Kulkarni, P., Baron, P. A., & Willeke, K. (2011). *Aerosol measurement : principles, techniques, and applications*. (3rd ed.). Hoboken, N.J. : Wiley. URL: `http://app.knovel.com/web/toc.v/cid:kpAMPTAE18`.

Kulmala, M. (2003). How Particles Nucleate and Grow. *Science*, *302*, 1000–1001. URL: `https://science.sciencemag.org/content/302/5647/1000`. doi:`10.1126/science.1090848`.

Kulmala, M., Kerminen, V. M., Petäjä, T., Ding, A. J., & Wang, L. (2017). Atmospheric gas-to-particle conversion: Why NPF events are observed in megacities? *Faraday Discussions*, *200*, 271–288. URL: `http://dx.doi.org/10.1039/C6FD00257A`. doi:`10.1039/c6fd00257a`.

Kulmala, M., Mordas, G., Petäjä, T., Grönholm, T., Aalto, P. P., Vehkamäki, H., Hienola, A. I., Herrmann, E., Sipilä, M., Riipinen, I., Manninen, H. E., Hämeri, K., Stratmann, F., Bilde, M., Winkler, P. M., Birmili, W., & Wagner, P. E. (2007). The condensation particle counter battery (CPCB): A new tool to investigate the activation properties of nanoparticles. *Journal of Aerosol Science*, *38*, 289–304. URL: `http://www.sciencedirect.com/science/article/pii/S0021850206002138`. doi:`https://doi.org/10.1016/j.jaerosci.2006.11.008`.

Kulmala, M., Petäjä, T., Ehn, M., Thornton, J., Sipilä, M., Worsnop, D. R., & Kerminen, V.-M. (2014). Chemistry of Atmospheric Nucleation: On the Recent Advances on Precursor Characterization and Atmospheric Cluster Composition in Connection with Atmospheric New Particle Formation. *Annual Review of Physical Chemistry*, *65*, 21–37. URL: `https://doi.org/10.1146/annurev-physchem-040412-110014`. doi:`10.1146/annurev-physchem-040412-110014`.

Kumar, M., Trabelsi, T., & Francisco, J. S. (2018). Can urea be a seed for aerosol particle formation in air? *The Journal of Physical Chemistry A*, *122*, 3261–3269. doi:`10.1021/acs.jpca.8b02189`.

Kupiainen-Määttä, O., Olenius, T., Kurtén, T., & Vehkamäki, H. (2013). Cims sulfuric acid detection efficiency enhanced by amines due to higher dipole moments: A computational study. *J. Phys. Chem. A*, *117*, 14109–14119. doi:`10.1021/jp4049764`.

Kürten, A., Bergen, A., Heinritzi, M., Leiminger, M., Lorenz, V., Piel, F., Simon, M., Sitals, R., Wagner, A. C., & Curtius, J. (2016). Observation of new particle formation and measurement of sulfuric acid, ammonia, amines and highly oxidized organic molecules at a rural site in central Germany. *Atmospheric Chemistry and Physics*, *16*, 12793–12813. URL: `https://acp.copernicus.org/articles/16/12793/2016/`. doi:`10.5194/acp-16-12793-2016`.

Kurtén, T., Hyttinen, N., D'Ambro, E. L., Thornton, J., & Prisle, N. L. (2018). Estimating the saturation vapor pressures of isoprene oxidation products $C_5H_{12}O_6$ and $C_5H_{10}O_6$ using cosmo-rs. *Atmospheric Chemistry and Physics*, *18*, 17589–17600. URL: `https://acp.copernicus.org/articles/18/17589/2018/`. doi:`10.5194/acp-18-17589-2018`.

Kurtén, T., Petäjä, T., Smith, J., Ortega, I. K., Sipilä, M., Junninen, H., Ehn, M., Vehkamäki, H., Mauldin, L., Worsnop, D. R., & Kulmala, M. (2011). The effect of h_2so_4–amine clustering on chemical ionization mass spectrometry (cims) measurements of gas-phase sulfuric acid. *Atmospheric Chemistry and Physics*, *11*, 3007–3019. URL: `https://www.atmos-chem-phys.net/11/3007/2011/`. doi:`10.5194/acp-11-3007-2011`.

Kurtén, T., Torpo, L., Ding, C.-G., Vehkamäki, H., Sundberg, M. R., Laasonen, K., & Kulmala, M. (2007). A density functional study on water-sulfuric acid-ammonia clusters and implications for atmospheric cluster formation. *J. Geophys. Res. Atmos.*, *112*, D04210. URL: `http://dx.doi.org/10.1029/2006JD007391`. doi:`10.1029/2006JD007391`.

Kurtén, T., Tiusanen, K., Roldin, P., Rissanen, M., Luy, J.-N., Boy, M., Ehn, M., & Donahue, N. (2016). α-pinene autoxidation products may not have extremely low saturation vapor pressures despite high o:c ratios. *The Journal of Physical Chemistry A*, *120*, 2569–2582. doi:`10.1021/acs.jpca.6b02196`.

Lane, T. E., Donahue, N. M., & Pandis, S. N. (2008). Simulating secondary organic aerosol formation using the volatility basis-set approach in a chemical transport model. *Atmospheric Environment*, *42*, 7439–7451.

Larsen, A. H., Mortensen, J. J., Blomqvist, J., Castelli, I. E., Christensen, R., Dułak, M., Friis, J., Groves, M. N., Hammer, B., Hargus, C., Hermes, E. D., Jennings, P. C., Jensen, P. B., Kermode, J., Kitchin, J. R., Kolsbjerg, E. L., Kubal, J., Kaasbjerg, K., Lysgaard, S., Maronsson, J. B., Maxson, T., Olsen, T., Pastewka, L., Peterson, A., Rostgaard, C., Schiøtz, J., Schütt, O., Strange, M., Thygesen, K. S., Vegge, T., Vilhelmsen, L., Walter, M., Zeng, Z., & Jacobsen, K. W. (2017). The atomic simulation environment—a python library for working with atoms. *Journal of Physics: Condensed Matter*, *29*, 273002. doi:`10.1088/1361-648x/aa680e`.

Lawler, M. J., Rissanen, M. P., Ehn, M., Mauldin, R. L., Sarnela, N., Sipilä, M., & Smith, J. N. (2018). Evidence for Diverse Biogeochemical Drivers of Boreal Forest New Particle Formation. *Geophysical Research Letters*, *45*, 2038–2046. doi:`10.1002/2017GL076394`.

Lee, S.-H., Uin, J., Guenther, A. B., de Gouw, J. A., Yu, F., Nadykto, A. B., Herb, J., Ng, N. L., Koss, A., Brune, W. H., Baumann, K., Kanawade, V. P., Keutsch, F. N., Nenes, A., Olsen, K., Goldstein, A., & Ouyang, Q. (2016). Isoprene suppression of new particle formation: Potential mechanisms and implications. *Journal of Geophysical Research: Atmospheres*, *121*, 14,621–14,635. URL: `https://agupubs.onlinelibrary.wiley.com/doi/abs/10.1002/2016JD024844`. doi:`10.1002/2016JD024844`. `arXiv:https://agupubs.onlinelibrary.wiley.com/doi/pdf/10.1002/2016JD024844`.

Leppä, J., Gagné, S., Laakso, L., Manninen, H. E., Lehtinen, K. E. J., Kulmala, M., & Kerminen, V.-M. (2013). Using measurements of the aerosol charging state in determination of the particle growth rate and the proportion of ion-induced nucleation. *Atmospheric Chemistry and Physics*, *13*, 463–486. URL: `https://www.atmos-chem-phys.net/13/463/2013/`. doi:`10.5194/acp-13-463-2013`.

Leverentz, H. R., Siepmann, J. I., Truhlar, D. G., Loukonen, V., & Vehkamäki, H. (2013). Energetics of atmospherically implicated clusters made of sulfuric acid, ammonia, and dimethyl amine. *J. Phys. Chem. A*, *117*, 3819–3825. URL: `http://dx.doi.org/10.1021/jp402346u`. doi:`10.1021/jp402346u`.

Li, H., Kupiainen-Määttä, O., Zhang, H., Zhang, X., & Ge, M. (2017). A molecular-scale study on the role of lactic acid in new particle formation: Influence of relative humidity and temperature. *Atmospheric Environment*, *166*, 479–487.

Li, H., Ning, A., Zhong, J., Zhang, H., Liu, L., Zhang, Y., Zhang, X., Zeng, X. C., & He, H. (2020). Influence of atmospheric conditions on sulfuric acid-dimethylamine-ammonia-based new particle formation. *Chemosphere*, *245*, 125554.

Lifson, S., & Warshel, A. (1968). Consistent force field for calculations of conformations, vibrational spectra, and enthalpies of cycloalkane and n-alkane molecules. *J. Chem. Phys.*, *49*, 5116–5129.

Liu, L., Kupiainen-Määttä, O., Zhang, H., Li, H., Zhong, J., Kurtén, T., Vehkamäki, H., Zhang, S., Zhang, Y., Ge, M., Zhang, X., & Li, Z. (2018a). Clustering mechanism of oxocarboxylic acids involving hydration reaction: Implications for the atmospheric models. *The Journal of Chemical Physics*, *148*, 214303. doi:`10.1063/1.5030665`.

Liu, L., Li, H., Zhang, H., Zhong, J., Bai, Y., Ge, M., Li, Z., Chen, Y., & Zhang, X. (2018b). The role of nitric acid in atmospheric new particle formation. *Physical Chemistry Chemical Physics*, *20*, 17406–17414.

Lopez-Hilfiker, F. D., Mohr, C., Ehn, M., Rubach, F., Kleist, E., Wildt, J., Mentel, T. F., Lutz, A., Hallquist, M., Worsnop, D., & Thornton, J. A. (2014). A novel method for online analysis of gas and particle composition: Description and evaluation of a filter inlet for gases and AEROsols (FIGAERO). *Atmospheric Measurement Techniques*, *7*, 983–1001. URL: `https://www.atmos-meas-tech.net/7/983/2014/`. doi:`10.5194/amt-7-983-2014`.

Lössl, P., Snijder, J., & Heck, A. J. (2014). Boundaries of mass resolution in native mass spectrometry. *Journal of the American Society for Mass Spectrometry*, *25*, 906–917. URL: `https://pubs.acs.org/doi/abs/10.1021/jasms.8b04794`. doi:`10.1007/s13361-014-0874-3`.

Loukonen, V., Kuo, I. W., McGrath, M., & Vehkamäki, H. (2014). On the stability and dynamics of (sulfuric acid)(ammonia) and (sulfuric acid)(dimethylamine) clusters: A first-principles molecular dynamics investigation. *Chemical Physics*, *428*, 164–174.

Loukonen, V., Kurtén, T., Ortega, I. K., Vehkamäki, H., Pádua, A. A. H., Sellegri, K., & Kulmala, M. (2010). Enhancing effect of dimethylamine in sulfuric acid nucleation in the presence of water – a computational study. *Atmos. Chem. Phys.*, *10*, 4961–4974. URL: `http://www.atmos-chem-phys.net/10/4961/2010/`. doi:`10.5194/acp-10-4961-2010`.

Low, K., Kobayashi, R., & Izgorodina, E. I. (2020). The effect of descriptor choice in machine learning models for ionic liquid melting point prediction. *The Journal of Chemical Physics*, *153*, 104101. doi:`10.1063/5.0016289`.

Ma, F., Xie, H.-B., Elm, J., Shen, J., Chen, J., & Vehkamäki, H. (2019). Piperazine enhancing sulfuric acid-based new particle formation: Implications for the atmospheric fate of piperazine. *Environmental Science & Technology*, *53*, 8785–8795. doi:`10.1021/acs.est.9b02117`.

Mäkelä, J., Hoffmann, T., Holzke, C., Väkevä, M., Suni, T., Mattila, T., Aalto, P., Tapper, U., Kauppinen, E. I., & O'Dowd, C. (2002). Biogenic iodine emissions and identification of end-products in coastal ultrafine particles during nucleation bursts. *Journal of Geophysical Research: Atmospheres*, *107*, PAR–14.

Mallina, R. V., Wexler, A. S., Rhoads, K. P., & Johnston, M. V. (2000). High Speed Particle Beam Generation: A Dynamic Focusing Mechanism for Selecting Ultrafine Particles. *Aerosol Science and Technology*, *33*, 87–104. URL: `https://doi.org/10.1080/027868200410868`. doi:`10.1080/027868200410868`.

Marple, V. A., Rubow, K. L., & Behm, S. M. (1991). A Microorifice Uniform Deposit impactor (MOUDI): Description, Calibration, and Use. *Aerosol Science and Technology*, *14*, 434–436. doi:`10.1080/02786829108959504`.

McGrath, M. J., Olenius, T., Ortega, I. K., Loukonen, V., Paasonen, P., Kurtén, T., Kulmala, M., & Vehkamäki, H. (2012). Atmospheric cluster dynamics code: a flexible method for solution of the birth–death equations. *Atmos. Chem. Phys.*, *12*, 2345–2355. URL: `http://www.atmos-chem-phys.net/12/2345/2012/`. doi:`10.5194/acp-12-2345-2012`.

McMurry, P. H., Ghimire, A., Ahn, H.-K., Sakurai, H., Moore, K., Stolzenburg, M., & Smith, J. N. (2009). Sampling nanoparticles for chemical analysis by low resolution electrical mobility classification. *Environmental Science & Technology*, *43*, 4653–4658. doi:`10.1021/es8029335`.

McMurry, P. H., Litchy, M., Huang, P. F., Cai, X., Turpin, B. J., Dick, W. D., & Hanson, A. (1996). Elemental composition and morphology of individual particles separated by size and hygroscopicity with the TDMA. *Atmospheric Environment*, *30*, 101–108. doi:`10.1016/1352-2310(95)00235-Q`.

McMurry, P. H., & Stolzenburg, M. R. (1989). On the sensitivity of particle size to relative humidity for Los Angeles aerosols. *Atmospheric Environment (1967)*, *23*, 497–507. doi:`10.1016/0004-6981(89)90593-3`.

Merikanto, J., Zapadinsky, E., Lauri, A., & Vehkamäki, H. (2007). Origin of the failure of classical nucleation theory: Incorrect description of the smallest clusters. *Phys. Rev. Lett.*, *98*, 145702.

Mohr, C., Thornton, J. A., Heitto, A., Lopez-Hilfiker, F. D., Lutz, A., Riipinen, I., Hong, J., Donahue, N. M., Hallquist, M., Petäjä, T. et al. (2019). Molecular identification of organic vapors driving atmospheric nanoparticle growth. *Nature communications*, *10*, 1–7.

Murphy, D. M., Cziczo, D. J., Froyd, K. D., Hudson, P. K., Matthew, B. M., Middlebrook, A. M., Peltier, R. E., Sullivan, A., Thomson, D. S., & Weber, R. J. (2006). Single-peptide mass spectrometry of tropospheric aerosol particles. *Journal of Geophysical Research Atmospheres*, *111*, 1–15. doi:`10.1029/2006JD007340`.

Myllys, N., Chee, S., Olenius, T., Lawler, M., & Smith, J. N. (2019a). Molecular-level understanding of synergistic effects in sulfuric acid–amine–ammonia mixed clusters. *J. Phys. Chem. A*, *123*, 2420–2425. doi:`10.1021/acs.jpca.9b00909`.

Myllys, N., Elm, J., Halonen, R., Kurtén, T., & Vehkamäki, H. (2016a). Coupled cluster evaluation of the stability of atmospheric acid–base clusters with up to 10 molecules. *J. Phys. Chem. A*, *120*, 621–630. doi:`10.1021/acs.jpca.5b09762`.

Myllys, N., Elm, J., & Kurtén, T. (2016b). Density functional theory basis set convergence of sulfuric acid-containing molecular clusters. *Comput. Theor. Chem.*, *1098*, 1–12. URL: `http://www.sciencedirect.com/science/article/pii/S2210271X16304297`. doi:`http://dx.doi.org/10.1016/j.comptc.2016.10.015`.

Myllys, N., Kubečka, J., Besel, V., Alfaouri, D., Olenius, T., Smith, J. N., & Passananti, M. (2019b). Role of base strength, cluster structure and charge in sulfuric-acid-driven particle formation. *Atmos. Chem. Phys.*, *19*, 9753–9768. URL: `https://www.atmos-chem-phys.net/19/9753/2019/`. doi:`10.5194/acp-19-9753-2019`.

Myllys, N., Olenius, T., Kurtén, T., Vehkamäki, H., Riipinen, I., & Elm, J. (2017). Effect of bisulfate, ammonia, and ammonium on the clustering of organic acids and sulfuric acid. *J. Phys. Chem. A*, *121*, 4812–4824. doi:`10.1021/acs.jpca.7b03981`.

Myllys, N., Ponkkonen, T., Chee, S., & Smith, J. (2020). Enhancing potential of trimethylamine oxide on atmospheric particle formation. *Atmosphere*, *11*, 35. URL: `http://dx.doi.org/10.3390/atmos11010035`. doi:`10.3390/atmos11010035`.

Myllys, N., Ponkkonen, T., Passananti, M., Elm, J., Vehkamäki, H., & Olenius, T. (2018). Guanidine: A highly efficient stabilizer in atmospheric new-particle formation. *J. Phys. Chem. A*, *122*, 4717–4729. doi:`10.1021/acs.jpca.8b02507`.

Mäkelä, J. M., Yli-Koivisto, S., Hiltunen, V., Seidl, W., Swietlicki, E., Teinila, K., Sillanpää, M., Koponen, I. K., Paatero, J., Rosman, K., & Hämeri, K. (2001). Chemical composition of aerosol during particle formation events in boreal forest. *Tellus B*, *53*, 380–393. URL: `http://dx.doi.org/10.1034/j.1600-0889.2001.530405.x`. doi:`10.1034/j.1600-0889.2001.530405.x`.

Nadykto, A. B., & Yu, F. (2007). Strong hydrogen bonding between atmospheric nucleation precursors and common organics. *Chem. Phys. Lett.*, *435*, 14–18. URL: `http://www.Sciencedirect.com/Science/article/pii/S0009261406018586`. doi:`http://dx.doi.org/10.1016/j.cplett.2006.12.050`.

Nadykto, A. B., Yu, F., Jakovleva, M. V., Herb, J., & Xu, Y. (2011). Amines in the earth's atmosphere: A density functional theory study of the thermochemistry of pre-nucleation clusters. *Entropy*, *13*, 554–569.

Neese, F. (2003). An improvement of the resolution of the identity approximation for the formation of the coulomb matrix. *J. Comp. Chem.*, *24*, 1740–1747.

Nielsen, C. J., D'Anna, B., Karl, M., Aursnes, M., Boreave, A., Bossi, R., Bunkan, A. J., Glasius, M., Hallquist, M., Hansen, A. M. K. et al. (2011). Atmospheric degradation of amines (ada): Summary report: Photo-oxidation of methylamine, dimethylamine and trimethylamine.

Ning, A., Zhang, H., Zhang, X., Li, Z., Zhang, Y., Xu, Y., & Ge, M. (2020). A molecular-scale study on the role of methanesulfinic acid in marine new particle formation. *Atmospheric Environment*, *227*, 117378. URL: `http://www.sciencedirect.com/science/article/pii/S1352231020301175`. doi:`https://doi.org/10.1016/j.atmosenv.2020.117378`.

Oberreit, D., Rawat, V. K., Larriba-Andaluz, C., Ouyang, H., McMurry, P. H., & Hogan, C. J. (2015). Analysis of heterogeneous water vapor uptake by metal iodide cluster ions via differential mobility analysis-mass spectrometry. *The Journal of Chemical Physics*, *143*, 104204. URL: `https://doi.org/10.1063/1.4930278`. doi:`10.1063/1.4930278`. `arXiv:https://doi.org/10.1063/1.4930278`.

O'Dowd, C. D., Aalto, P., Hämeri, K., Kulmala, M., & Hoffmann, T. (2002). Atmospheric particles from organic vapours. *Nature*, *416*, 497–498. URL: `www.nature.com`. doi:`10.1038/416497a`.

Olenius, T., Halonen, R., Kurtén, T., Henschel, H., Kupiainen-Määttä, O., Ortega, I. K., Jen, C. N., Vehkamäki, H., & Riipinen, I. (2017). New particle formation from sulfuric acid and amines: Comparison of mono-, di-, and trimethylamines. *J. Geophys. Res. Atmos.*, *122*, 7103–7118. URL: `http://dx.doi.org/10.1002/2017JD026501`. doi:`10.1002/2017JD026501`.

Olenius, T., Kupiainen-Määttä, O., Ortega, I. K., Kurtén, T., & Vehkamäki, H. (2013). Free energy barrier in the growth of sulfuric acid–ammonia and sulfuric acid–dimethylamine clusters. *J. Chem. Phys.*, *139*, 084312.

URL: `http://scitation.aip.org/content/aip/journal/jcp/139/8/10.1063/1.4819024`. doi:`http://dx.doi.org/10.1063/1.4819024`.

Olenius, T., Yli-Juuti, T., Elm, J., Kontkanen, J., & Riipinen, I. (2018). Chapter 11 - new particle formation and growth: Creating a new atmospheric phase interface. In J. A. Faust, & J. E. House (Eds.), *Physical Chemistry of Gas-Liquid Interfaces* Developments in Physical & Theoretical Chemistry (pp. 315 – 352). Elsevier. URL: `http://www.sciencedirect.com/science/article/pii/B978012813641600011X`. doi:`https://doi.org/10.1016/B978-0-12-813641-6.00011-X`.

Ortega, I. K., Donahue, N. M., Kurtén, T., Kulmala, M., Focsa, C., & Vehkamäki, H. (2016). Can highly oxidized organics contribute to atmospheric new particle formation? *The Journal of Physical Chemistry A*, *120*, 1452–1458. doi:`10.1021/acs.jpca.5b07427`.

Ortega, I. K., Kupiainen, O., Kurtén, T., Olenius, T., Wilkman, O., McGrath, M. J., Loukonen, V., & Vehkamäki, H. (2012). From quantum chemical formation free energies to evaporation rates. *Atmos. Chem. Phys.*, *12*, 225–235. URL: `http://www.atmos-chem-phys.net/12/225/2012/`. doi:`10.5194/acp-12-225-2012`.

Ortega, I. K., Kurtén, T., Vehkamäki, H., & Kulmala, M. (2008). The role of ammonia in sulfuric acid ion induced nucleation. *Atmos. Chem. Phys.*, *8*, 2859–2867. URL: `http://www.atmos-chem-phys.net/8/2859/2008/`. doi:`10.5194/acp-8-2859-2008`.

Ortega, I. K., Olenius, T., Kupiainen-Määttä, O., Loukonen, V., Kurtén, T., & Vehkamäki, H. (2014). Electrical charging changes the composition of sulfuric acid–ammonia/dimethylamine clusters. *Atmos. Chem. Phys.*, *14*, 7995–8007. URL: `https://www.atmos-chem-phys.net/14/7995/2014/`. doi:`10.5194/acp-14-7995-2014`.

Öström, E., Putian, Z., Schurgers, G., Mishurov, M., Kivekäs, N., Lihavainen, H., Ehn, M., Rissanen, M. P., Kurtén, T., Boy, M., Swietlicki, E., & Roldin, P.

(2017). Modeling the role of highly oxidized multifunctional organic molecules for the growth of new particles over the boreal forest region. *Atmospheric Chemistry and Physics*, *17*, 8887–8901. URL: `https://acp.copernicus.org/articles/17/8887/2017/`. doi:`10.5194/acp-17-8887-2017`.

Ouyang, H., He, S., Larriba-Andaluz, C., & Hogan, C. J. (2015). Ims–ms and ims–ims investigation of the structure and stability of dimethylamine-sulfuric acid nanoclusters. *The Journal of Physical Chemistry A*, *119*, 2026–2036. URL: `https://doi.org/10.1021/jp512645g`. doi:`10.1021/jp512645g`. `arXiv:https://doi.org/10.1021/jp512645g`. PMID: 25692213.

Pankow, J. F., & Asher, W. E. (2008). Simpol.1: a simple group contribution method for predicting vapor pressures and enthalpies of vaporization of multifunctional organic compounds. *Atmospheric Chemistry and Physics*, *8*, 2773–2796. URL: `https://www.atmos-chem-phys.net/8/2773/2008/`. doi:`10.5194/acp-8-2773-2008`.

Partanen, L., Hänninen, V., & Halonen, L. (2012). Ab initio structural and vibrational investigation of sulfuric acid monohydrate. *The Journal of Physical Chemistry A*, *116*, 2867–2879. doi:`10.1021/jp210489f`.

Partanen, L., Pesonen, J., Sjöholm, E., & Halonen, L. (2013). A rotamer energy level study of sulfuric acid. *The Journal of Chemical Physics*, *139*, 144311. doi:`10.1063/1.4823836`.

Partanen, L., Vehkamäki, H., Hansen, K., Elm, J., Henschel, H., Kurtén, T., Halonen, R., & Zapadinsky, E. (2016). Effect of conformers on free energies of atmospheric complexes. *The Journal of Physical Chemistry A*, *120*, 8613–8624. doi:`10.1021/acs.jpca.6b04452`.

Passananti, M., Zapadinsky, E., Zanca, T., Kangasluoma, J., Myllys, N., Rissanen, M. P., Kurtén, T., Ehn, M., Attoui, M., & Vehkamäki, H. (2019). How well can we predict cluster fragmentation inside a mass spectrometer? *Chemical Communications*, *55*, 5946–5949.

Pennington, M. R., & Johnston, M. V. (2012). Trapping charged nanoparticles in the nano aerosol mass spectrometer (NAMS). *International Journal of Mass Spectrometry*, *311*, 64–71. doi:`10.1016/j.ijms.2011.12.011`.

Perraud, V., Li, X., Jiang, J., Finlayson-Pitts, B. J., & Smith, J. N. (2020a). Size-Resolved Chemical Composition of Sub-20 nm Particles from Methanesulfonic Acid Reactions with Methylamine and Ammonia. *ACS Earth and Space Chemistry*, . doi:`10.1021/acsearthspacechem.0c00120`.

Perraud, V., Xu, J., Gerber, R. B., & Finlayson-Pitts, B. (2020b). Integrated experimental and theoretical approach to probe the synergistic effect of ammonia in methanesulfonic acid reactions with small alkylamines. *Environmental Science: Processes & Impacts*, *22*, 305–328.

Pihlajamäki, A., Hämäläinen, J., Linja, J., Nieminen, P., Malola, S., Kärkkäinen, T., & Häkkinen, H. (2020). Monte carlo simulations of au38(sch3)24 nanocluster using distance-based machine learning methods. *The Journal of Physical Chemistry A*, *124*, 4827–4836. doi:`10.1021/acs.jpca.0c01512`.

Rader, D. J., & McMurry, P. H. (1986). Application of the tandem differential mobility analyzer to studies of droplet growth or evaporation. *Journal of Aerosol Science*, *17*, 771–787. doi:`10.1016/0021-8502(86)90031-5`.

Rasmussen, F. R., Kubečka, J., Besel, V., Vehkamäki, H., Mikkelsen, K. V., Bilde, M., & Elm, J. (2020). Hydration of Atmospheric Molecular Clusters III: Procedure for Efficient Free Energy Surface Exploration of Large Hydrated Clusters. *The Journal of Physical Chemistry A*, *124*, 5253–5261. URL: `https://doi.org/10.1021/acs.jpca.0c02932`. doi:`10.1021/acs.jpca.0c02932`.

Renzler, M., Kranabetter, L., Goulart, M., Scheier, P., & Echt, O. (2017). Positively and Negatively Charged Cesium and (C60)mCsn Cluster Ions. *Journal of Physical Chemistry C*, *121*, 10817–10823. URL: `https://doi.org/10.1021/acs.jpcc.6b11928`. doi:`10.1021/acs.jpcc.6b11928`.

Riplinger, C., Pinski, P., Becker, U., Valeev, E. F., & Neese, F. (2016). Sparse maps—a systematic infrastructure for reduced-scaling electronic structure methods. ii. linear scaling domain based pair natural orbital coupled cluster theory. *J. Chem. Phys.*, *144*, 024109. doi:`10.1063/1.4939030`.

Riplinger, C., Sandhoefer, B., Hansen, A., & Neese, F. (2013). Natural triple excitations in local coupled cluster calculations with pair natural orbitals. *J. Chem. Phys.*, *139*, 134101. URL: `http://scitation.aip.org/content/aip/journal/jcp/139/13/10.1063/1.4821834`. doi:`http://dx.doi.org/10.1063/1.4821834`.

Roldin, P., Ehn, M., Kurtén, T., Olenius, T., Rissanen, M. P., Sarnela, N., Elm, J., Rantala, P., Hao, L., Hyttinen, N. et al. (2019). The role of highly oxygenated organic molecules in the boreal aerosol-cloud-climate system. *Nature communications*, *10*, 1–15.

Roldin, P., Eriksson, A. C., Nordin, E. Z., Hermansson, E., Mogensen, D., Rusanen, A., Boy, M., Swietlicki, E., Svenningsson, B., Zelenyuk, A., & Pagels, J. (2014). Modelling non-equilibrium secondary organic aerosol formation and evaporation with the aerosol dynamics, gas- and particle-phase chemistry kinetic multilayer model adcham. *Atmospheric Chemistry and Physics*, *14*, 7953–7993. URL: `https://acp.copernicus.org/articles/14/7953/2014/`. doi:`10.5194/acp-14-7953-2014`.

Roldin, P., Liao, L., Mogensen, D., Dal Maso, M., Rusanen, A., Kerminen, V.-M., Mentel, T. F., Wildt, J., Kleist, E., Kiendler-Scharr, A., Tillmann, R., Ehn, M., Kulmala, M., & Boy, M. (2015). Modelling the contribution of biogenic volatile organic compounds to new particle formation in the jülich plant atmosphere chamber. *Atmospheric Chemistry and Physics*, *15*, 10777–10798. URL: `https://acp.copernicus.org/articles/15/10777/2015/`. doi:`10.5194/acp-15-10777-2015`.

Roldin, P., Swietlicki, E., Schurgers, G., Arneth, A., Lehtinen, K. E. J., Boy, M., & Kulmala, M. (2011). Development and evaluation of the aerosol dynamics and gas phase chemistry model adchem. *Atmospheric Chemistry and Physics*, *11*, 5867–5896. URL: https://acp.copernicus.org/articles/11/5867/2011/. doi:10.5194/acp-11-5867-2011.

Rose, C., Zha, Q., Dada, L., Yan, C., Lehtipalo, K., Junninen, H., Mazon, S. B., Jokinen, T., Sarnela, N., Sipilä, M., Petäjä, T., Kerminen, V.-M., Bianchi, F., & Kulmala, M. (2018). Observations of biogenic ion-induced cluster formation in the atmosphere. *Science Advances*, *4*, eaar5218. URL: http://advances.sciencemag.org/content/4/4/eaar5218.abstract. doi:10.1126/sciadv.aar5218.

Roudsari, G., Reischl, B., Pakarinen, O. H., & Vehkamäki, H. (2020). Atomistic simulation of ice nucleation on silver iodide (0001) surfaces with defects. *The Journal of Physical Chemistry C*, *124*, 436–445. doi:10.1021/acs.jpcc.9b08502.

Rupp, M., Tkatchenko, A., Müller, K.-R., & von Lilienfeld, O. A. (2012). Fast and accurate modeling of molecular atomization energies with machine learning. *Phys. Rev. Lett.*, *108*, 058301. URL: https://link.aps.org/doi/10.1103/PhysRevLett.108.058301. doi:10.1103/PhysRevLett.108.058301.

Sakurai, H., Fink, M. A., McMurry, P. H., Mauldin, L., Moore, K. F., Smith, J. N., & Eisele, F. L. (2005). Hygroscopicity and volatility of 4-10 nm particles during summertime atmospheric nucleation events in urban Atlanta. *Journal of Geophysical Research Atmospheres*, *110*, 1–10. URL: http://doi.wiley.com/10.1029/2005JD005918. doi:10.1029/2005JD005918.

Sarnela, N., Jokinen, T., Nieminen, T., Lehtipalo, K., Junninen, H., Kangasluoma, J., Hakala, J., Taipale, R., Schobesberger, S., Sipilä, M., Larnimaa, K., Westerholm, H., Heijari, J., Kerminen, V.-M., Petäjä, T., & Kulmala, M. (2015). Sulphuric acid and aerosol particle production in the vicinity of an oil refinery. *Atmospheric Environment*, *119*, 156–166. URL: http://www.sciencedirect.com/science/article/pii/S1352231015302788. doi:https://doi.org/10.1016/j.atmosenv.2015.08.033.

Schmitz, G., & Elm, J. (2020). Assessment of the dlpno binding energies of strongly noncovalent bonded atmospheric molecular clusters. *ACS Omega*, *5*, 7601–7612. doi:`10.1021/acsomega.0c00436`.

Schobesberger, S., Junninen, H., Bianchi, F., Lönn, G., Ehn, M., Lehtipalo, K., Dommen, J., Ehrhart, S., Ortega, I. K., Franchin, A., Nieminen, T., Riccobono, F., Hutterli, M., Duplissy, J., Almeida, J., Amorim, A., Breitenlechner, M., Downard, A. J., Dunne, E. M., Flagan, R. C., Kajos, M., Keskinen, H., Kirkby, J., Kupc, A., Kürten, A., Kurtén, T., Laaksonen, A., Mathot, S., Onnela, A., Praplan, A. P., Rondo, L., Santos, F. D., Schallhart, S., Schnitzhofer, R., Sipilä, M., Tomé, A., Tsagkogeorgas, G., Vehkamäki, H., Wimmer, D., Baltensperger, U., Carslaw, K. S., Curtius, J., Hansel, A., Petäjä, T., Kulmala, M., Donahue, N. M., & Worsnop, D. R. (2013). Molecular understanding of atmospheric particle formation from sulfuric acid and large oxidized organic molecules. *Proc. Natl. Acad. Sci.*, *110*, 17223–17228. URL: `http://www.pnas.org/content/110/43/17223.abstract`. doi:`10.1073/pnas.1306973110`. `arXiv:http://www.pnas.org/content/110/43/17223.full.pdf`.

Seinfeld, J. H., Pandis, S. N., & Noone, K. (1998). *Atmospheric Chemistry and Physics: From Air Pollution to Climate Change*. (3rd ed.). Hoboken: John Wiley & Sons, Inc. doi:`10.1063/1.882420`.

Shen, J., Xie, H.-B., Elm, J., Ma, F., Chen, J., & Vehkamäki, H. (2019). Methanesulfonic acid-driven new particle formation enhanced by monoethanolamine: A computational study. *Environmental Science & Technology*, *53*, 14387–14397. doi:`10.1021/acs.est.9b05306`.

Shiraiwa, M., Pfrang, C., Koop, T., & Pöschl, U. (2012). Kinetic multi-layer model of gas-particle interactions in aerosols and clouds (km-gap): linking condensation, evaporation and chemical reactions of organics, oxidants and water. *Atmospheric Chemistry and Physics*, *12*, 2777–2794. URL: `https://acp.copernicus.org/articles/12/2777/2012/`. doi:`10.5194/acp-12-2777-2012`.

Shiraiwa, M., Pfrang, C., & Pöschl, U. (2010). Kinetic multi-layer model of aerosol surface and bulk chemistry (km-sub): the influence of interfacial transport and bulk diffusion on the oxidation of oleic acid by ozone. *Atmospheric Chemistry and Physics*, *10*, 3673–3691. URL: `https://acp.copernicus.org/articles/10/3673/2010/`. doi:`10.5194/acp-10-3673-2010`.

Silva, P. J., Erupe, M. E., Price, D., Elias, J., G. J. Malloy, Q., Li, Q., Warren, B., & Cocker, D. R. (2008). Trimethylamine as precursor to secondary organic aerosol formation via nitrate radical reaction in the atmosphere. *Environ. Sci. Technol.*, *42*, 4689–4696. doi:`10.1021/es703016v`.

Sipilä, M., Lehtipalo, K., Attoui, M., Neitola, K., Petäjä, T., Aalto, P. P., O'Dowd, C. D., & Kulmala, M. (2009). Laboratory Verification of PH-CPC's Ability to Monitor Atmospheric Sub-3 nm Clusters. *Aerosol Science and Technology*, *43*, 126–135. URL: `http://www.tandfonline.com/doi/abs/10.1080/02786820802506227`. doi:`10.1080/02786820802506227`.

Sipilä, M., Sarnela, N., Jokinen, T., Henschel, H., Junninen, H., Kontkanen, J., Richters, S., Kangasluoma, J., Franchin, A., Peräkylä, O., Rissanen, M. P., Ehn, M., Vehkamäki, H., Kurten, T., Berndt, T., Petäjä, T., Worsnop, D., Ceburnis, D., Kerminen, V.-M., Kulmala, M., & O'Dowd, C. (2016). Molecular-scale evidence of aerosol particle formation via sequential addition of HIO3. *Nature*, *537*, 532–534. URL: `https://doi.org/10.1038/nature19314`. doi:`10.1038/nature19314`.

Sipilä, M., Sarnela, N., Jokinen, T., Junninen, H., Hakala, J., Rissanen, M. P., Praplan, A., Simon, M., Kürten, A., Bianchi, F., Dommen, J., Curtius, J., Petäjä, T., & Worsnop, D. R. (2015). Bisulfate-cluster based atmospheric pressure chemical ionization mass spectrometer for high-sensitivity ($<$ 100 ppqv) detection of atmospheric dimethyl amine: proof-of-concept and first ambient data from boreal forest. *Atmospheric Measurement Techniques*, *8*, 4001–4011. URL: `https://www.atmos-meas-tech.net/8/4001/2015/`. doi:`10.5194/amt-8-4001-2015`.

Smith, J. N., Barsanti, K. C., Friedli, H. R., Ehn, M., Kulmala, M., Collins, D. R., Scheckman, J. H., Williams, B. J., & McMurry, P. H. (2010). Observations of aminium salts in atmospheric nanoparticles and possible climatic implications. *Proceedings of the National Academy of Sciences of the United States of America*, *107*, 6634–6639. URL: `http://www.pnas.org/cgi/doi/10.1073/pnas.0912127107http://www.pnas.org/content/107/15/6634.abstract{%}5Cnhttp://www.pnas.org/content/107/15/6634.full.pdf`. doi:`10.1073/pnas.0912127107`.

Smith, J. N., Moore, K. F., McMurry, P. H., & Eisele, F. L. (2004). Atmospheric Measurements of Sub-20 nm Diameter Particle Chemical Composition by Thermal Desorption Chemical Ionization Mass Spectrometry. *Aerosol Science and Technology*, *38*, 100–110. URL: `http://www.tandfonline.com/doi/abs/10.1080/02786820490249036`. doi:`10.1080/02786820490249036`.

Smith, J. N., & Rathbone, G. J. (2008). Carboxylic acid characterization in nanoparticles by thermal desorption chemical ionization mass spectrometry. *International Journal of Mass Spectrometry*, *274*, 8–13. URL: `http://www.sciencedirect.com/science/article/pii/S1387380608001371`. doi:`10.1016/j.ijms.2008.04.008`.

Stangl, C. M., & Johnston, M. V. (2017). Aqueous Reaction of Dicarbonyls with Ammonia as a Potential Source of Organic Nitrogen in Airborne Nanoparticles. *Journal of Physical Chemistry A*, *121*, 3720–3727. URL: `https://doi.org/10.1021/acs.jpca.7b02464`. doi:`10.1021/acs.jpca.7b02464`.

Temelso, B., Archer, K. A., & Shields, G. C. (2011). Benchmark structures and binding energies of small water clusters with anharmonicity corrections. *The Journal of Physical Chemistry A*, *115*, 12034–12046.

Temelso, B., Klein, K. L., Mabey, J. W., Pérez, C., Pate, B. H., Kisiel, Z., & Shields, G. C. (2018a). Exploring the rich potential energy surface of (h2o)

11 and its physical implications. *Journal of chemical theory and computation*, *14*, 1141–1153.

Temelso, B., Morrell, T. E., Shields, R. M., Allodi, M. A., Wood, E. K., Kirschner, K. N., Castonguay, T. C., Archer, K. A., & Shields, G. C. (2012). Quantum mechanical study of sulfuric acid hydration: Atmospheric implications. *The Journal of Physical Chemistry A*, *116*, 2209–2224.

Temelso, B., Morrison, E. F., Speer, D. L., Cao, B. C., Appiah-Padi, N., Kim, G., & Shields, G. C. (2018b). Effect of mixing ammonia and alkylamines on sulfate aerosol formation. *J. Phys. Chem. A*, *122*, 1612–1622. doi:`10.1021/acs.jpca.7b11236`.

Temelso, B., & Shields, G. C. (2011). The role of anharmonicity in hydrogen-bonded systems: The case of water clusters. *Journal of chemical theory and computation*, *7*, 2804–2817.

Thomas, J. M., He, S., Larriba-Andaluz, C., DePalma, J. W., Johnston, M. V., & Hogan Jr., C. J. (2016). Ion mobility spectrometry-mass spectrometry examination of the structures, stabilities, and extents of hydration of dimethylamine–sulfuric acid clusters. *Phys. Chem. Chem. Phys.*, *18*, 22962–22972. URL: `http://dx.doi.org/10.1039/C6CP03432B`. doi:`10.1039/C6CP03432B`.

Toivola, M., Napari, I., & Vehkamäki, H. (2009). Structure of water–sulfuric acid clusters from molecular dynamics simulations. *Boreal Environ. Res.*, (p. 654).

Toivola, M., Prisle, N. L., Elm, J., Waxman, E. M., Volkamer, R., & Kurtén, T. (2017). Can cosmotherm predict a salting in effect? *The Journal of Physical Chemistry A*, *121*, 6288–6295. doi:`10.1021/acs.jpca.7b04847`.

Tsagkogeorgas, G., Roldin, P., Duplissy, J., Rondo, L., Tröstl, J., Slowik, J. G., Ehrhart, S., Franchin, A., Kürten, A., Amorim, A., Bianchi, F., Kirkby, J., Petäjä, T., Baltensperger, U., Boy, M., Curtius, J., Flagan, R. C., Kulmala, M., Donahue, N. M., & Stratmann, F. (2017). Evaporation of sulfate aerosols at low relative humidity. *Atmospheric Chemistry and Physics*, *17*, 8923–8938. URL: `https://acp.copernicus.org/articles/17/8923/2017/`. doi:`10.5194/acp-17-8923-2017`.

Vaattovaara, P., Räsänen, M., Kühn, T., Joutsensaari, J., & Laaksonen, A. (2005). A method for detecting the presence of organic fraction in nucleation mode sized particles. *Atmospheric Chemistry and Physics*, *5*, 3277–3287. URL: `https://acp.copernicus.org/articles/5/3277/2005/`. doi:`10.5194/acp-5-3277-2005`.

Vaida, V. (2011). Perspective: Water cluster mediated atmospheric chemistry. *The Journal of Chemical Physics*, *135*, 020901. doi:`10.1063/1.3608919`.

Vaida, V., Kjaergaard, H. G., & Feierabend, K. J. (2003). Hydrated complexes: Relevance to atmospheric chemistry and climate. *International Reviews in Physical Chemistry*, *22*, 203–219. doi:`10.1080/0144235031000075780`.

Vehkamäki, H. (2006). *Classical nucleation theory in multicomponent systems*. Springer Science & Business Media.

Vehkamäki, H., & Riipinen, I. (2012). Thermodynamics and kinetics of atmospheric aerosol particle formation and growth. *Chem. Soc. Rev.*, *41*, 5160–5173. URL: `http://dx.doi.org/10.1039/C2CS00002D`. doi:`10.1039/C2CS00002D`.

Visser, T. (2002). FT-IR detection in gas chromatography. *TrAC Trends in Analytical Chemistry*, *21*, 627–636. URL: `http://www.sciencedirect.com/science/article/pii/S0165993602008129`. doi:`https://doi.org/10.1016/S0165-9936(02)00812-9`.

Voisin, D., Smith, J. N., Sakurai, H., McMurry, P. H., & Eisele, F. L. (2003). Thermal desorption chemical ionization mass spectrometer for ultrafine particle chemical composition. *Aerosol Science and Technology*, *37*, 471–475. doi:`10.1080/02786820300959`.

Wagner, A. C., Bergen, A., Brilke, S., Fuchs, C., Ernst, M., Hoker, J., Heinritzi, M., Simon, M., Bühner, B., Curtius, J., & Kürten, A. (2018). Size-resolved online chemical analysis of nanoaerosol particles: A thermal desorption differential mobility analyzer coupled to a chemical ionization time-of-flight mass spectrometer. *Atmospheric Measurement Techniques*, *11*, 5489–5506. doi:`10.5194/amt-11-5489-2018`.

Wagner, R., Yan, C., Lehtipalo, K., Duplissy, J., Nieminen, T., Kangasluoma, J., Ahonen, L. R., Dada, L., Kontkanen, J., Manninen, H. E., Dias, A., Amorim, A., Bauer, P. S., Bergen, A., Bernhammer, A. K., Bianchi, F., Brilke, S., Buenrostro Mazon, S., Chen, X., Draper, D. C., Fischer, L., Frege, C., Fuchs, C., Garmash, O., Gordon, H., Hakala, J., Heikkinen, L., Heinritzi, M., Hofbauer, V., Hoyle, C. R., Kirkby, J., Kürten, A., Kvashnin, A. N., Laurila, T., Lawler, M. J., Mai, H., Makhmutov, V., Mauldin, R., Molteni, U., Nichman, L., Nie, W., Ojdanic, A., Onnela, A., Piel, F., Quéléver, L. L., Rissanen, M. P., Sarnela, N., Schallhart, S., Sengupta, K., Simon, M., Stolzenburg, D., Stozhkov, Y., Tröstl, J., Viisanen, Y., Vogel, A. L., Wagner, A. C., Xiao, M., Ye, P., Baltensperger, U., Curtius, J., Donahue, N. M., Flagan, R. C., Gallagher, M., Hansel, A., Smith, J. N., Tomé, A., Winkler, P. M., Worsnop, D., Ehn, M., Sipilä, M., Kerminen, V. M., Petäjä, T., & Kulmala, M. (2017). The role of ions in new particle formation in the CLOUD chamber. *Atmospheric Chemistry and Physics*, *17*, 15181–15197. URL: `https://www.atmos-chem-phys-discuss.net/acp-2017-536/`. doi:`10.5194/acp-17-15181-2017`.

Wang, C., Seames, W. S., Gadgil, M., Hrdlicka, J., & Fix, G. (2007). Comparison of coal ash particle size distributions from Berner and Dekati low pressure impactors. *Aerosol Science and Technology*, *41*, 1049–1062. doi:`10.1080/02786820701697788`.

Wang, C.-Y., Jiang, S., Liu, Y.-R., Wen, H., Wang, Z.-Q., Han, Y.-J., Huang, T., & Huang, W. (2018). Synergistic effect of ammonia and methylamine on nucleation in the earth's atmosphere. a theoretical study. *J. Phys. Chem. A*, *122*, 3470–3479. doi:`10.1021/acs.jpca.8b00681`.

Wang, M., Kong, W., Marten, R., He, X. C., Chen, D., Pfeifer, J., Heitto, A., Kontkanen, J., Dada, L., Kürten, A., Yli-Juuti, T., Manninen, H. E., Amanatidis, S., Amorim, A., Baalbaki, R., Baccarini, A., Bell, D. M., Bertozzi, B., Bräkling, S., Brilke, S., Murillo, L. C., Chiu, R., Chu, B., De Menezes, L. P., Duplissy, J., Finkenzeller, H., Carracedo, L. G., Granzin, M., Guida, R., Hansel, A., Hofbauer, V., Krechmer, J., Lehtipalo, K., Lamkaddam, H., Lampimäki, M., Lee, C. P., Makhmutov, V., Marie, G., Mathot, S., Mauldin, R. L., Mentler, B., Müller, T., Onnela, A., Partoll, E., Petäjä, T., Philippov, M., Pospisilova, V., Ranjithkumar, A., Rissanen, M., Rörup, B., Scholz, W., Shen, J., Simon, M., Sipilä, M., Steiner, G., Stolzenburg, D., Tham, Y. J., Tomé, A., Wagner, A. C., Wang, D. S., Wang, Y., Weber, S. K., Winkler, P. M., Wlasits, P. J., Wu, Y., Xiao, M., Ye, Q., Zauner-Wieczorek, M., Zhou, X., Volkamer, R., Riipinen, I., Dommen, J., Curtius, J., Baltensperger, U., Kulmala, M., Worsnop, D. R., Kirkby, J., Seinfeld, J. H., El-Haddad, I., Flagan, R. C., & Donahue, N. M. (2020). Rapid growth of new atmospheric particles by nitric acid and ammonia condensation. *Nature*, *581*, 184–189. URL: `https://doi.org/10.1038/s41586-020-2270-4`. doi:`10.1038/s41586-020-2270-4`.

Wang, S., Zordan, C. A., & Johnston, M. V. (2006). Chemical characterization of individual, airborne sub-10-nm particles and molecules. *Analytical Chemistry*, *78*, 1750–1754. URL: `http://dx.doi.org/10.1021/ac052243l`. doi:`10.1021/ac052243l`.

Wang, Z., Su, H., Wang, X., Ma, N., Wiedensohler, A., Pöschl, U., & Cheng, Y. (2015). Scanning supersaturation condensation particle counter applied as a nano-CCN counter for size-resolved analysis of the hygroscopicity and chemical composition of nanoparticles. *Atmospheric Measurement Techniques*, *8*, 2161–2172. URL: `https://amt.copernicus.org/articles/8/2161/2015/`. doi:`10.5194/amt-8-2161-2015`.

Warshel, A., & Levitt, M. (1976). Theoretical studies of enzymic reactions: Dielectric, electrostatic and steric stabilization of the carbonium ion in the reaction of lysozyme. *Journal of Molecular Biology*, *103*, 227 – 249. URL: `http://www.sciencedirect.com/science/article/pii/0022283676903119`. doi:`https://doi.org/10.1016/0022-2836(76)90311-9`.

Wu, Z. (2017). Gain Insight into Chemical Components Driving New Particle Growth on a Basis of Particle Hygroscopicity and Volatility Measurements: a Short Review. *Current Pollution Reports*, *3*, 175–181. URL: `https://doi.org/10.1007/s40726-017-0064-6`. doi:`10.1007/s40726-017-0064-6`.

Xie, H.-B., Elm, J., Halonen, R., Myllys, N., Kurtén, T., Kulmala, M., & Vehkamäki, H. (2017). Atmospheric fate of monoethanolamine: Enhancing new particle formation of sulfuric acid as an important removal process. *Environ. Sci. Technol.*, *51*, 8422–8431. doi:`10.1021/acs.est.7b02294`.

Xu, J., Finlayson-Pitts, B. J., & Gerber, R. B. (2017). Proton transfer in mixed clusters of methanesulfonic acid, methylamine, and oxalic acid: Implications for atmospheric particle formation. *The Journal of Physical Chemistry A*, *121*, 2377–2385.

Xu, J., Perraud, V., Finlayson-Pitts, B. J., & Gerber, R. B. (2018). Uptake of water by an acid–base nanoparticle: theoretical and experimental studies of the methanesulfonic acid–methylamine system. *Physical Chemistry Chemical Physics*, *20*, 22249–22259.

Xu, W., & Zhang, R. (2012). Theoretical investigation of interaction of dicarboxylic acids with common aerosol nucleation precursors. *The Journal of Physical Chemistry A*, *116*, 4539–4550. doi:`10.1021/jp301964u`.

Xu, Y., Nadykto, A. B., Yu, F., Herb, J., & Wang, W. (2010a). Interaction between common organic acids and trace nucleation species in the earth's atmosphere. *J. Phys. Chem. A*, *114*, 387–396. doi:`10.1021/jp9068575`.

Xu, Y., Nadykto, A. B., Yu, F., Jiang, L., & Wang, W. (2010b). Formation and properties of hydrogen-bonded complexes of common organic oxalic acid with atmospheric nucleation precursors. *J. Mol. Struc.: THEOCHEM*, *951*, 28–33.

Yang, H., Goudeli, E., & Hogan, C. J. (2018). Condensation and dissociation rates for gas phase metal clusters from molecular dynamics trajectory calculations. *The Journal of Chemical Physics*, *148*, 164304. doi:`10.1063/1.5026689`.

Yao, L., Garmash, O., Bianchi, F., Zheng, J., Yan, C., Kontkanen, J., Junninen, H., Mazon, S. B., Ehn, M., Paasonen, P., Sipilä, M., Wang, M., Wang, X., Xiao, S., Chen, H., Lu, Y., Zhang, B., Wang, D., Fu, Q., Geng, F., Li, L., Wang, H., Qiao, L., Yang, X., Chen, J., Kerminen, V.-M., Petäjä, T., Worsnop, D. R., Kulmala, M., & Wang, L. (2018). Atmospheric new particle formation from sulfuric acid and amines in a Chinese megacity. *Science*, *361*, 278 LP – 281. URL: `http://science.sciencemag.org/content/361/6399/278.abstract`. doi:`10.1126/science.aao4839`.

Yli-Juuti, T., Barsanti, K., Hildebrandt Ruiz, L., Kieloaho, A.-J., Makkonen, U., Petäjä, T., Ruuskanen, T., Kulmala, M., & Riipinen, I. (2013). Model for acid-base chemistry in nanoparticle growth (mabnag). *Atmospheric Chemistry and Physics*, *13*, 12507–12524. URL: `https://www.atmos-chem-phys.net/13/12507/2013/`. doi:`10.5194/acp-13-12507-2013`.

Yu, H., McGraw, R., & Lee, S.-H. (2012). Effects of amines on formation of sub-3 nm particles and their subsequent growth. *Geophys. Res. Lett.*, *39*, L02807.

Yue, G. K., & Hamill, P. (1979). The homogeneous nucleation rates of h2so4-h2o aerosol particles in air. *J. Aerosol Sci.*, *10*, 609–614. URL: `http://www.Sciencedirect.com/Science/article/pii/0021850279900235`. doi:`http://dx.doi.org/10.1016/0021-8502(79)90023-5`.

Zapadinsky, E., Passananti, M., Myllys, N., Kurtén, T., & Vehkamäki, H. (2019). Modeling on fragmentation of clusters inside a mass spectrometer. *J. Phys. Chem. A*, *123*, 611–624. doi:`10.1021/acs.jpca.8b10744`.

Zhang, H., Kupiainen-Määttä, O., Zhang, X., Molinero, V., Zhang, Y., & Li, Z. (2017). The enhancement mechanism of glycolic acid on the formation of atmospheric sulfuric acid–ammonia molecular clusters. *The Journal of Chemical Physics*, *146*, 184308.

Zhang, H., Li, H., Liu, L., Zhang, Y., Zhang, X., & Li, Z. (2018). The potential role of malonic acid in the atmospheric sulfuric acid-ammonia clusters formation. *Chemosphere*, *203*, 26–33.

Zhang, J., & Dolg, M. (2015). Abcluster: The artificial bee colony algorithm for cluster global optimization. *Phys. Chem. Chem. Phys.*, *17*, 24173–24181. URL: `http://dx.doi.org/10.1039/C5CP04060D`. doi:`10.1039/C5CP04060D`.

Zhang, J., & Dolg, M. (2016). Global optimization of clusters of rigid molecules using the artificial bee colony algorithm. *Phys. Chem. Chem. Phys.*, *18*, 3003–3010. URL: `http://dx.doi.org/10.1039/C5CP06313B`. doi:`10.1039/C5CP06313B`.

Zhang, J., Glezakou, V.-A., Rousseau, R., & Nguyen, M.-T. (2020). Nwpesse: An adaptive-learning global optimization algorithm for nanosized cluster systems. *Journal of Chemical Theory and Computation*, *16*, 3947–3958. doi:`10.1021/acs.jctc.9b01107`.

Zhang, R., Wang, L., Khalizov, A. F., Zhao, J., Zheng, J., Mcgraw, R. L., & Molina, L. T. (2009). Formation of nanoparticles of blue haze enhanced by anthropogenic pollution. *Proceedings of the National Academy of Sciences of the United States of America*, *106*, 17650–17654.

Zhang, R. Y., Khalizov, A., Wang, L., Hu, M., & Xu, W. (2012). Nucleation and growth of nanoparticles in the atmosphere. *Chemical Reviews*, *112*, 1957–2011. doi:`10.1021/cr2001756`.

Zhao, J., Eisele, F. L., Titcombe, M., Kuang, C., & McMurry, P. H. (2010). Chemical ionization mass spectrometric measurements of atmospheric neutral clusters using the cluster-CIMS. *Journal of Geophysical Research*, *115*, D08205. doi:`10.1029/2009jd012606`.

Zordan, C. A., Wang, S., & Johnston, M. V. (2008). Time-Resolved Chemical Composition of Individual Nanoparticles in Urban Air. *Environmental Science & Technology*, *42*, 6631–6636. URL: `https://doi.org/10.1021/es800880z`. doi:`10.1021/es800880z`.

James Smith is a professor of chemistry at the University of California, Irvine (UCI). His research focuses on performing laboratory and field measurements in order to understand and quantify the mechanisms of atmospheric nanoparticle formation and growth. He received his PhD in 2000 from the California Institute of Technology and was a research scientist at the National Center for Atmospheric Research from 2000-2015.

Danielle Draper is an atmospheric chemist with interests in volatile organic compound (VOC) oxidation mechanisms and secondary organic aerosol (SOA) formation processes from combined biogenic and anthropogenic sources. Her work combines theoretical calculations, laboratory experiments, and in situ observations. She is currently a graduate student in the Smith group at UCI and expects to receive her PhD at the end of 2020. She will be starting a postdoc at Caltech in 2021.

Sabrina Chee is currently a Chemistry PhD graduate student in the Smith group at UCI. Her research focuses on the driving forces behind the formation and growth of salt nanoparticles via reactive uptake of gaseous acids and bases. She measures lab-nucleated particle composition (<20 nm) with the TDCIMS.

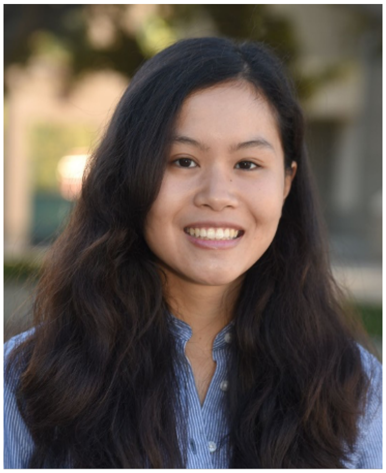

Michelia Dam is a graduate student studying new particle formation in the Smith group at UCI. Her research probes organic oxidation chemistry in experimental chamber studies to gain gas phase mechanistic insight and assess particle formation potential.

Hayley Glicker obtained her Bachelor of Science degree in Chemistry from Mills College in spring of 2016 and began her PhD degree in the Smith group at UCI the following fall. Her research focuses on characterizing ultrafine particle composition in remote atmospheres: the Amazon basin and marine environments.

Deanna Myers received her BSc in Chemistry from Western Washington University and is currently a PhD student in the Smith group at UCI. Her research is focused on laboratory and field studies of atmospheric particle formation and properties, particularly interactions with water vapor.

Adam Thomas obtained his BSc in chemistry at the University of California, Riverside in 2018, and is currently a graduate student researcher in the Smith group at UCI. Adam's research interests are centered around the application of high-resolution mass spectrometry for the analysis of organic aerosol particle composition.

Michael Lawler is an atmospheric chemist and earth system scientist with interests in aerosol formation and biosphere-atmosphere interactions, particularly in remote regions of the troposphere. He received his PhD from University of California, Irvine, in 2011 and rejoined UCI recently as a project scientist in the Smith group. He has made in situ observations of trace atmospheric constituents in many locations around the globe.

Nanna Myllys obtained BSc, MSc and PhD degrees from the University of Helsinki and is currently a postdoc in the Smith group at UCI. Nanna is a theoretical chemist studying clustering, reaction mechanisms and particle properties. Her research focuses on the development of a reactive cluster formation and growth models based on first principles. In 2021 she will start a new position at the University of Jyväskylä, which will combine computational and spectroscopic approaches to studies of atmospheric complexes.